Strengthening of the Air Quality Information System

Working area 2: Application of a regional-scale model over the central part of Chile

-

REGIONAL DISPERSION OF OXIDIZED SULFUR OVER CENTRAL CHILE: A SUMMER CASE

L. Gallardo, G. Olivares and A. Aguayo
National Commission for the Environment, Chile
and
J. Langner and B. Århus
Swedish Meteorological and Hydrological Institute, Sweden

December 1999

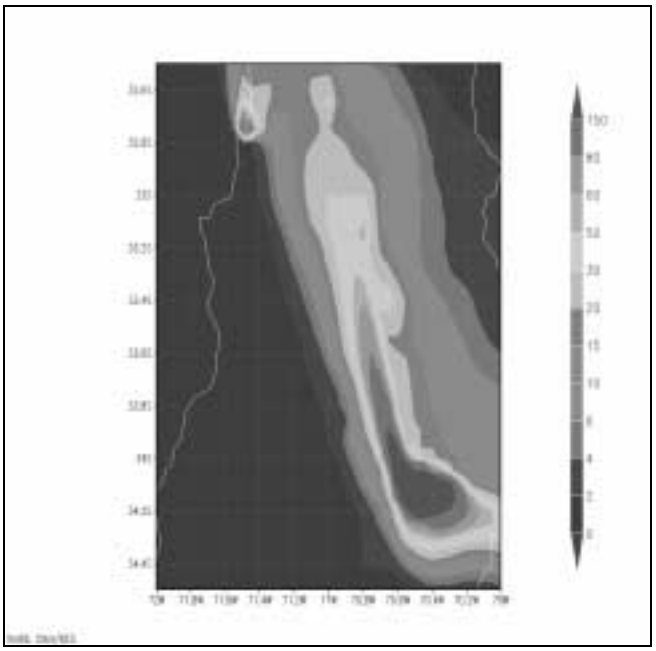

Oxidized sulfur over Central Chile for January 17 1998
as simulated by HIRLAM-MATCH

DISPERSIÓN REGIONAL DE AZUFRE OXIDADO EN CHILE CENTRAL: UN CASO DE VERANO

L. Gallardo, G. Olivares y A. Aguayo

Comisión Nacional del Medio Ambiente, Chile

y

J. Langner y B. Århus

Instituto Sueco de Meteorología e Hidrología, Suecia

RESUMEN

En los últimos años, se han realizado esfuerzos para establecer inventarios de emisiones, redes de monitoreo meteorológicas y de calidad del aire en zonas urbanas, especialmente en Santiago. Estos datos empiezan a hacer posible la aplicación de herramientas de modelación atmosférica de mesoescala y de escala regional. Aquí se presenta un primer intento para evaluar la distribución regional de contaminantes de origen antrópico, principalmente compuestos oxidados de azufre, en Chile central. La dispersión de estos compuestos es simulada con un modelo Euleriano de área limitada, "*off-line*" (MATCH). Los patrones meteorológicos de Chile central son simulados a través de un modelo meteorológico de área limitada (HIRLAM). Analizamos en particular un escenario de verano correspondiente a Enero de 1998. Esta evaluación será complementada por varias pruebas que se harán para escenarios de primavera, otoño e invierno y que se presentarán en futuros informes.

Los datos meteorológicos producidos por la actual configuración de HIRLAM se estiman como suficientemente precisos para la simulación de la dispersión regional de contaminantes en Chile central. Simulaciones más detalladas para Santiago requieren la inclusión de los efectos meteorológicos de la ciudad, por ejemplo, efectos derivados de la isla calórica y la rugosidad provocados por la ciudad. Una mayor resolución horizontal también se hace necesaria para simular efectos topográficos locales.

A escala regional, las emisiones de las fundiciones de cobre dominan el contenido de azufre oxidado en la atmósfera de Chile central. El predominio de las fundiciones aparece tanto en las distribuciones horizontal como vertical de los campos de azufre oxidado. Las emisiones urbanas tienen un impacto menor, inferior al 10%, sobre los contenidos de azufre fuera de las zonas urbanas y por sobre la capa de mezcla atmosférica si se compara con el impacto de las fundiciones. Además, las fundiciones contribuyen episódicamente a los contenidos de azufre de las urbes en conexión con la fuerte mezcla vertical que ocurre en las tardes estivales. Las simulaciones muestran también que existe una recirculación de las emisiones de Santiago siguiendo los vientos derivados del calentamiento diferencial entre las laderas de los cerros y el valle. De acuerdo a los vientos predominantes, en horas del día las grandes emisiones de contaminantes primarios (por ejemplo, monóxido de carbono) que ocurren en el centro de la ciudad son transportadas hacia y acumuladas en el oriente de Santiago. Durante la noche, cuando los vientos cambian de dirección, los contaminantes son transportados hacia la zona poniente.

El sistema de modelación (HIRLAM-MATCH) es capaz de reproducir, salvo efectos locales, las características principales del ciclo diurno de las concentraciones de monóxido de carbono (CO) y dióxido de azufre (SO_2) que muestran las observaciones disponibles en Chile central. Para dar cuenta de los efectos locales, se necesita de inventarios emisiones detallados y datos topográficos de usos de suelos de mayor resolución. A futuro, continuará la validación sistemática del modelo para situaciones con condiciones de perturbaciones subsinópticas como bajas costeras y perturbaciones de escala sinóptica como pasos frontales. También se evaluarán los módulos químicos.

REGIONAL DISPERSION OF OXIDIZED SULFUR OVER CENTRAL CHILE: A SUMMER CASE

L. Gallardo, G. Olivares and A. Aguayo

National Commission for the Environment, Chile

and

J. Langner and B. Århus

Swedish Meteorological and Hydrological Institute, Sweden

ABSTRACT

In the last years, efforts have been made for establishing emission inventories, meteorological and air quality networks in urban areas, especially in Santiago. These data begin to make modeling applications for meso- and regional scale problems a meaningful exercise. Here we present a first attempt to assess the regional distribution of man-made pollutants, mainly oxidized sulfur, in Central Chile. The dispersion of oxidized sulfur is simulated with a limited area, off-line, Eulerian transport model (MATCH). The meteorological features of Central Chile are modeled through a meteorological limited area model (HIRLAM). In particular, we analyze a summer scenario for January 1998. This evaluation will be complemented by several tests, which will be performed for spring, fall and winter scenarios in the up-coming reports.

For simulations of regional dispersion of air pollutants in the area of central Chile the meteorological data produced by the current set up of HIRLAM is judged to be sufficiently accurate. For detailed simulations of the dispersion of air pollutants in Santiago additional work is needed to include the influence of the city on the meteorological conditions, e.g. heat island and roughness effects. A higher horizontal resolution is also required to simulate small-scale topographic effects.

On the regional scale, the emissions of the copper smelters dominate the oxidized sulfur burden in Central Chile. The predominance of the copper sources appears both in horizontal and vertical distributions. The urban emissions have a modest impact, i.e., less than 10%, on the sulfur burden outside the urban areas, and above the mixed layer in comparison with the copper smelters. Moreover, the smelters contribute on an episodic basis to the sulfur burden in the urban areas in connection with strong vertical mixing in the afternoon hours. Also, over Santiago a recycling of the urban emissions related to the air movements caused by the up and down-slope winds driven by radiation are apparent from the simulations. Accordingly with the prevailing winds, during daytime the large primary emissions of pollutants (e.g., carbon monoxide) that take place in Central Santiago are transported towards and accumulated in Eastern Santiago. During night, when the winds turn to down-slope winds, the pollutants are transported westwards.

The modeling system (HIRLAM-MATCH) is able to reproduce, except for local effects the major features of the diurnal cycle as known in the available observations of carbon monoxide (CO) and sulfur dioxide (SO_2) in Central Chile. To account for local effects detailed emission inventories, topography and land-use data should be required. Future work will continue the systematic validation of the modeling tool in order to assess the model's performance under conditions of subsynoptical disturbances such as coastal lows and large-scale disturbances such as frontal passages. Also, the chemical modules will be tested.

1. INTRODUCTION

The economical development that Chile faces has consequences on the environment such as air pollution on local and regional scales. Strong measures are required to prevent and curb these problems. In this context, there is an increasing demand from policy makers to develop tools for the evaluation and assessment of anthropogenic impact on the atmosphere. Models, which describe emissions, transport, chemistry and deposition processes of the atmospheric constituents are one of the tools that must be developed for that purpose.

Until the mid 90's, the modeling tools most frequently applied for environmental assessments in Chile were Gaussian models developed by the Environmental Protection Agency of the United States. The majority of such applications considered the dispersion of sulfur dioxide (SO_2) and inhalable particulate matter (PM_{10}) in the surroundings of stationary sources, mainly within the intensive copper mining industry. In the last years, efforts have been made for establishing emission inventories, meteorological and air quality networks in urban areas, especially in Santiago. These data begin to make modeling applications for meso- and regional scale problems a meaningful exercise.

Through this project, we attempt to assess the regional distribution of man-made pollutants, mainly oxidized sulfur, in Central Chile. The dispersion of oxidized sulfur is simulated with a limited area, off-line, Eulerian transport model (MATCH). The meteorological features of Central Chile are modeled through a meteorological limited area model (HIRLAM).

In the following pages, a first evaluation of the model for the summer scenario of January 1998 is presented. The exercise we present must be understood as a step in the validation of a complex modeling tool for assessing the regional dispersion of pollutants. This first systematic evaluation will be complemented by several tests, which will be performed for spring, fall and winter scenarios in the up-coming reports.

In Section 2, the evaluation of the meteorological model (HIRLAM) is presented. In Section 3 the corresponding evaluation for the dispersion model (MATCH) is shown. The overall conclusions are summarized in Section 4.

2. METEOROLOGICAL SIMULATIONS (HIRLAM)

J. Langner and B. Århus

Swedish Meteorological and Hydrological Institute, Sweden

In order to provide the necessary meteorological input to model simulations of air pollutants over central Chile, the HIRLAM model, a three-dimensional dynamical meteorological model, has been set up for the area of Chile. The intention is to run HIRLAM for a number of one-month periods that cover different meteorological conditions relevant for study of the distribution of air pollutants in the region. Here we report details of the set up of the model and results for the period of January 1998.

2.1. The HIRLAM model

The HIRLAM (High Resolution Limited Area Model) is the result of a co-operation between the meteorological institutes in Denmark, Finland, Iceland, Ireland, The Netherlands, Norway, Spain and Sweden. There is also research co-operation with Météo-France (France). Most of the participants use the HIRLAM numerical weather prediction system, partly or in its entirety, in their local routine weather forecasting procedures. The aim of the HIRLAM project is to develop and maintain a numerical short-range weather forecasting system for operational use by the participating institutes. The co-operation started in 1985. Since 1 January 1997 the project is in its fourth phase, HIRLAM-4. A reference version of HIRLAM is maintained at the European Centre for Medium range Weather Forecasts (ECMWF), and all changes to HIRLAM are introduced via the reference system. Each HIRLAM member can obtain new versions via their links to ECMWF.

The basic forecasting model is a hydrostatic grid-point model and the resolutions presently in use are 55 to 5 km horizontally and 16 to 31 levels in the vertical. The coordinate systems used are a rotated latitude-longitude grid horizontally and a hybrid p-sigma system in the vertical. The time stepping is semi-implicit, Eulerian or semi-Lagrangian, and a fourth order, linear horizontal diffusion is used. The radiation scheme has been developed in the HIRLAM project, vertical diffusion is formulated through first order closure scheme and condensational processes are handled by the Sundqvist scheme. Surface processes are handled in a two-layer scheme with snow, ice and soil moisture included.

In addition to the basic forecast model, the HIRLAM system consists of an analysis scheme, an implicit, adiabatic normal mode initialization scheme and a post processing, diagnostics and verification package. In order to start a forecast an initial state for the prognostic variables in the model is produced by the analysis scheme. The analysis is made for surface pressure, atmospheric temperature, wind, and humidity as well as for sea surface temperature, ice and snow coverage. The analysis is adjusted by the initialization scheme to provide a balanced atmospheric state to start the model integration from. Apart from the initial state the model also requires boundary conditions along the lateral boundaries of the simulation domain. Such boundary conditions are usually taken from a global numerical weather prediction model e.g. the ECMWF global model.

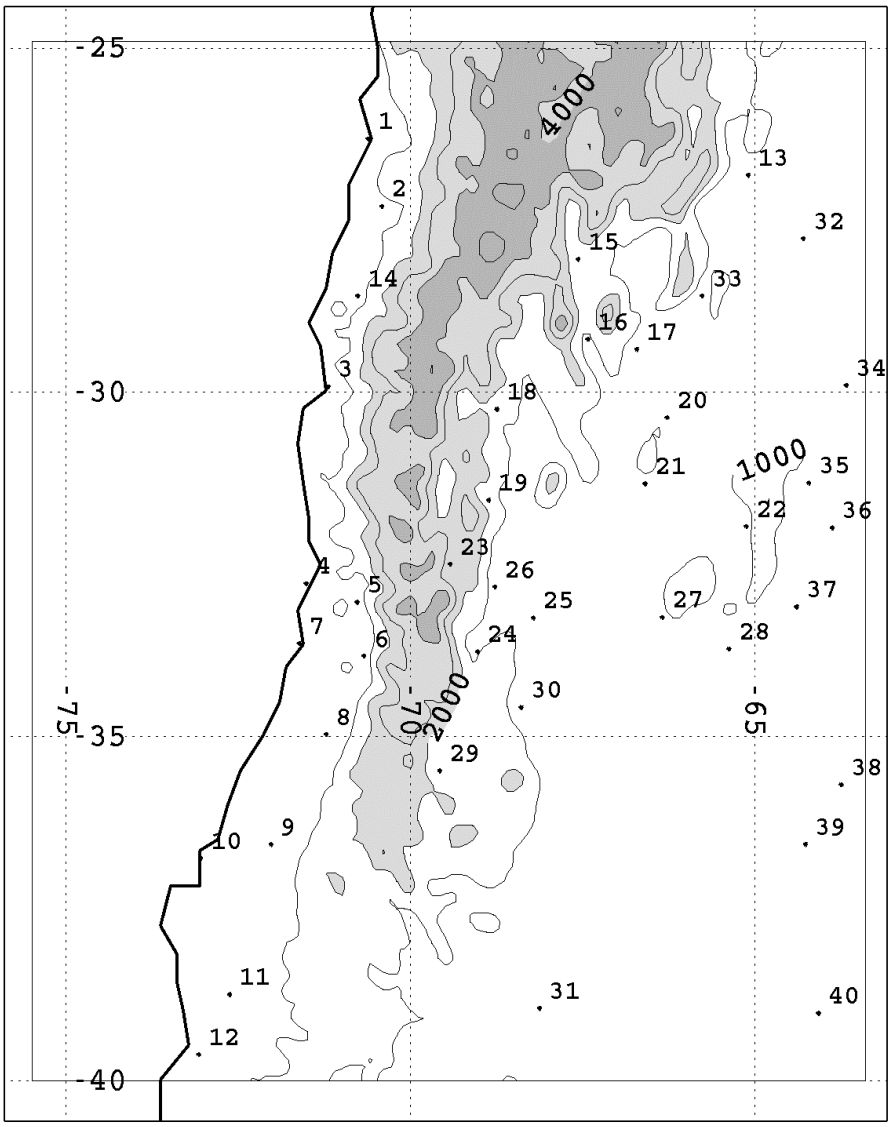

Figure 2.1. The model domain and WMO-stations from Table 2.2.

2.2. Set-up of HIRLAM for Chile

Since the focus of the present project is on historic periods rather than forecasts, the set-up of HIRLAM for Chile was done in a different way compared to what is used in routine weather prediction. Instead of running HIRLAM in an intermittent data assimilation cycle with repeated short-range (24-48 hour) forecasts the model was integrated continuously for about a one-month period only changing the lateral boundary conditions. This means that

the analysis and initialization schemes were not used. Instead the model is used as a dynamical downscaling tool to provide a more detailed representation of small-scale meteorological variations using a more coarse resolution forcing on the lateral boundaries. This approach has been shown to be successful for different kinds of climate applications over Europe. The main assumption that is made in this approach is that the model, which is used for forcing via the lateral boundary conditions, captures the important synoptic scale features.

The first test simulations were performed for the period of January 1998. This period is in the summer in the Southern Hemisphere. The period was chosen because of the strong diurnal variations in wind direction and speed that was evident from observations in the area of main interest. This should be a good test of the HIRLAM model. This period is also dry in the central Chile region and the complexities introduced by clouds and precipitation are therefore of limited importance during this period (at least over central Chile).

Six hourly boundary conditions from the ECMWF operational model at 0.5°x0.5° and 31 levels were used. The configuration of the vertical coordinate system in HIRLAM was identical to the one in the ECMWF data in order to avoid interpolation errors. The configuration of the levels is given in Table 2.1. Sea surface temperature (SST) was also taken from ECMWF at six-hour intervals. A regular latitude longitude grid was used in the horizontal direction. Several test runs were performed at different resolutions ranging from 0.2° (~22 km) to 0.05° (~5 km) horizontal resolution. The results presented here were all derived using a 0.1° (~11 km) horizontal resolution. The model domain had 122x152 grid points horizontally and the integration time step was used 180 s using semi Lagrangian timestepping. The model domain is shown in Figure 2.1.

2.3. Results

2.3.1. Synoptic meteorological conditions

The synoptic conditions in the area simulated are dominated by the South Pacific subtropical anticyclone which causes mostly southerly surface winds to the west of the Andes along the coast of Chile and dry and stable conditions. To the east of the Andes, the low-level circulation is mostly cyclonic as a result of a heat-low over the continent. During January 1998 the weather was dry, with little cloudiness to the west of the Andes range. There was no precipitation over central Chile during the period. However, a few synoptic disturbances with increased cloudiness traveled from southwest over the central Chile area during the period. Figure 2.2 shows maps of surface wind and cloud cover as simulated by HIRLAM for four different times during January 1998. Also shown is wind and cloudiness from available synoptic observations. Figure 2.3 shows the record of two-meter temperature and 10-meter wind speed observed at La Platina (M01, Table 2.5.), which is a meteorological station, located in an agricultural area in the southern part of Santiago. The record shows a strong diurnal cycle in temperature and wind speed. This is caused by the interaction of the prevailing southerly winds and radiatively driven up slope and down slope winds along the Andes during clear sky conditions. During daytime winds are up slope due to rapid heating of the mountainsides and during nighttime the wind is down slope due to cooling. The wind direction changes accordingly with southwesterly wind

during daytime and easterly winds during nighttime (not shown). An illustration of how HIRLAM predicts these diurnal changes over the Santiago region is given in Figure 2.4 which shows the surface wind field at midnight and local noon on the first of January 1998. Both the up slope and down slope winds are clearly visible. In the following we will make more detailed comparisons between the model simulations and available observations.

Table 2.1. Approximate level configuration in HIRLAM.

Level / Layer	Height (m)	Thickness (m)
1	32	64
2	144	460
3	344	240
4	614	300
5	696	345
6	1061	385
7	1461	415
8	1889	440
9	2339	460
10	2806	475
11	3289	490
12	3786	505
13	4301	525
14	4834	540
15	5386	565
16	5959	580
17	6549	600
18	7161	625
19	7801	655
20	8474	690
21	9184	730
22	9936	775
23	10741	835
24	11611	905
25	12561	995
26	13624	1130
27	14856	1335
28	16374	1700
29	18451	2455
30	21881	4405
31	26374	4580

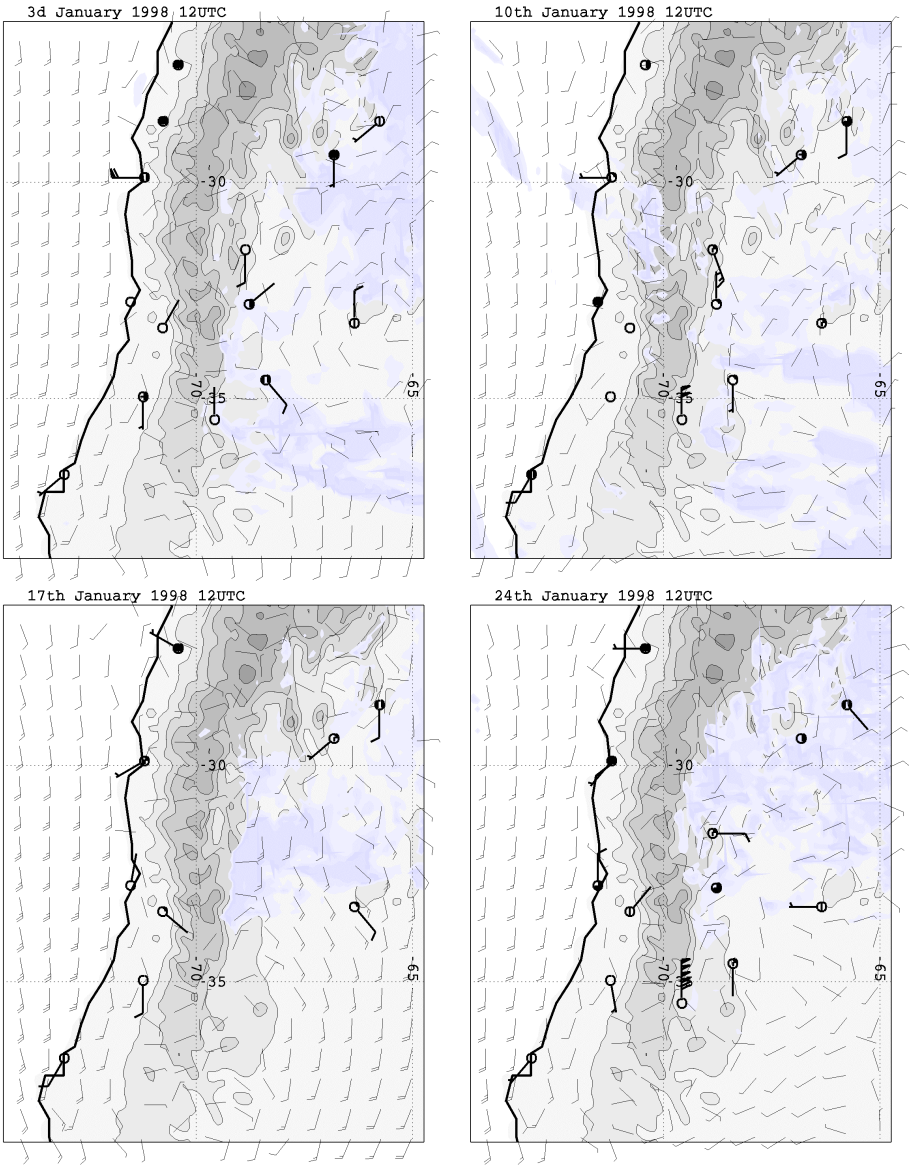

Figure 2.2. Maps of surface wind (10 meter) and cloud cover as simulated by HIRLAM for four different times during January 1998. Also shown is wind and cloud cover from available synoptic observations. The wind barb denotes wind speed and direction. The barb points in the direction the wind is blowing from. Speed is given in knots where half a barb represents 5 kts and a whole barb 10 kts. 2 kts is equal to 1 m/s. Note that the winds observed at the station close 35°S, 70°W seems to be in error.

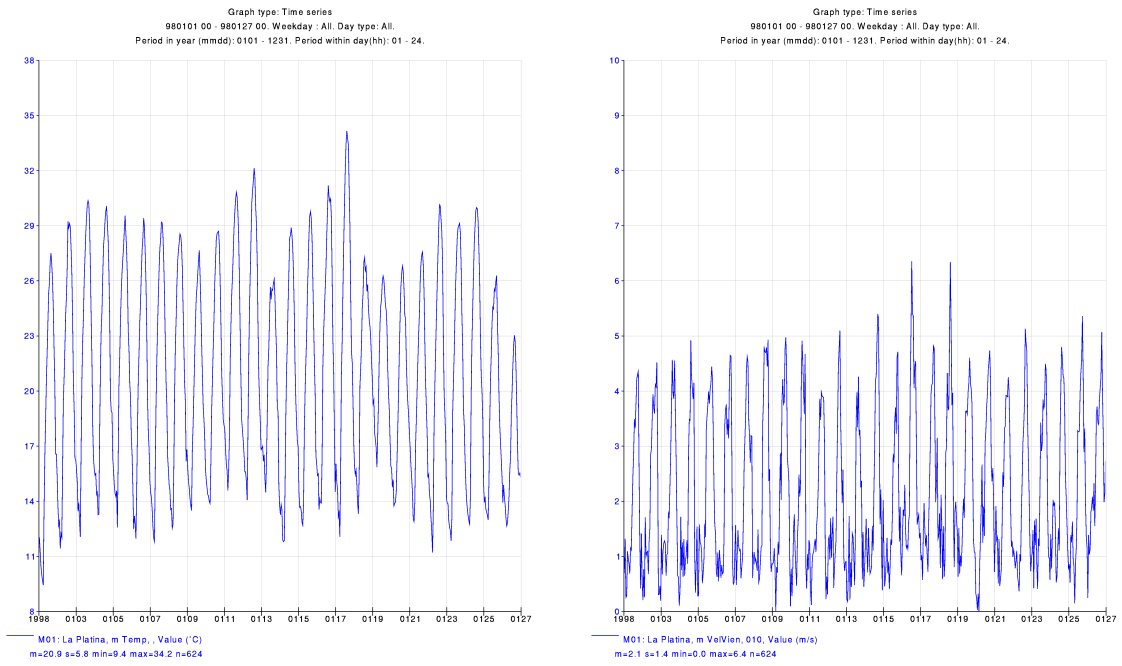

Figure 2.3 Observed temperature at two meter and wind speed at 10 meter at La Platina (M01). Units: °C and m/s.

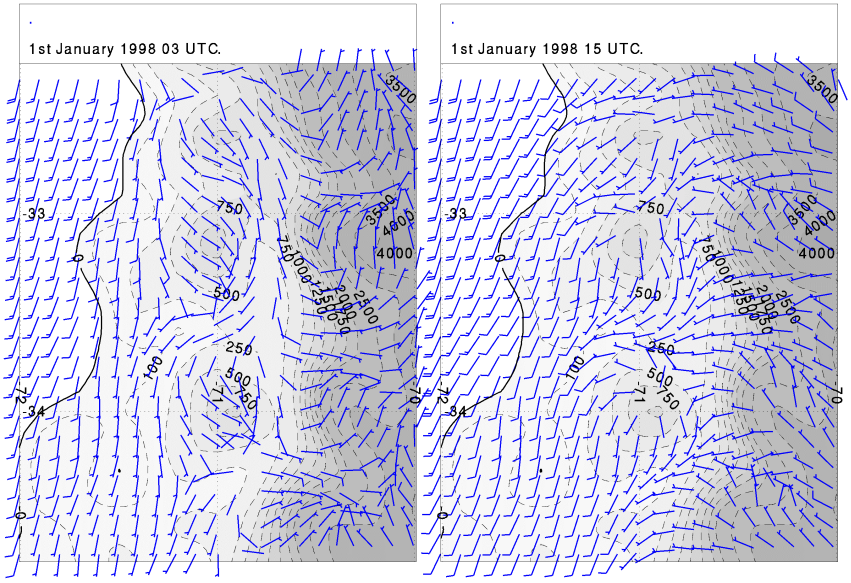

Figure 2.4. Maps of surface wind (10 meter) as simulated by HIRLAM over central Chile for 03 and 15 UTC (00 and 12 local time) on the first of January 1998. The wind barb denotes wind speed and direction. The barb points in the direction the wind is blowing from. Speed is given in knots where half a barb represents 5 kts and a whole barb 10 kts. 2 kts is equal to 1 m/s.

2.3.2. Comparison with routine meteorological measurements

In January 1998 data was available from 40 routine, synoptic meteorological stations, and three sounding stations within the model domain. These stations report data to the World Meteorological Organization (WMO) Global Telecommunications Network (GTS). Observations are usually made every third or six hour. Soundings are made twice a day at the sounding stations. The locations of the stations are given in Figure 2.1. Further information about the stations is given in Table 2.2. For the stations we have calculated the Root Mean Square difference (RMS) between the HIRLAM simulations and the observations as well as the bias in order to describe how well the HIRLAM model simulations agree with the observations. These measures describe the mean difference and tendency to over- or under-prediction. The result is given in Table 2.3 for the synoptic stations and in Table 2.4 for the sounding stations. In these calculations it was decided not to use the WMO-stations east for 65°W, because they are close to the boundary of the simulation domain of the HIRLAM model. To provide a reference the same comparisons were made for the analysis from ECMWF that was used as boundary conditions for the HIRLAM simulations. As the tables 2.3 and 2.4 show, the HIRLAM results are better than the ECMWF analysis for the synoptic stations for all parameters examined except for cloud cover which is better in the ECMWF analysis. This is not surprising since clouds are one of the parameters that are most difficult to simulate correctly. For the three sounding stations (Table 2.4) the ECMWF model has better results, in particular at the higher levels, while the results for 850 hPa are comparable. Again this is not very surprising since the soundings usually have a strong impact on the analysis. In conclusion the application of HIRLAM improves the description of the meteorological conditions compared to the ECMWF analysis near the surface except in the case of cloudiness. At upper levels the ECMWF analysis is closer to observations but the difference between HIRLAM and the observations is not much larger.

2.3.3. Comparison with meteorological measurements in the Santiago area

To evaluate the performance of HIRLAM in the region of central Chile, comparisons were made with observations from the network of meteorological stations run by CENMA (Centro Nacional del Medio Ambiente). The network consists of 25 stations. The location of the stations is shown in Figure 2.5. Some characteristics are given in Table 2.5. In addition to these stations the synoptic station at Santiago airport (Pudahuel) is also included in the comparison. It should be recognized that the network run by CENMA was designed in part to capture small-scale meteorological variations induced by the very complex topography in the region. Some of the stations are located in narrow valleys or close to small-scale topographic features. HIRLAM was set up with a horizontal grid distance of 11 km. The resulting representation of the topography (Figure 2.5) is still very smooth and many small-scale topographic features cannot be resolved.

Table 2.2. WMO-stations used in the evaluation. The three stations typeset in bold are also sounding stations. See also Figure 2.1.

Station	Index number	Name	Latitude	Longitude	Elevation (m)
1.	85460	Chanaral	-26.19	-70.37	30
2.	85470	Copiapo	-27.18	-70.25	290
3.	85488	La Serena	-29.54	-71.12	142
4.	**85543**	**Quintero Santiago**	**-32.47**	**-71.31**	**8**
5.	85574	Pudahuel	-33.23	-70.47	475
6.	85577	Santiago Q. Normal	-33.26	-70.41	520
7.	85586	Santo Domingo	-33.39	-71.37	75
8.	85629	Curico	-34.58	-71.14	228
9.	85672	Chillan	-36.34	-72.02	124
10.	85682	Concepcion	-36.46	-73.03	12
11.	85743	Temuco	-38.45	-72.38	114
12.	85766	Valdivia	-39.37	-73.05	19
13.	87121	Tucuman Aero	-26.51	-65.06	440
14.	85486	Vallenar	-28.36	-70.46	526
15.	87211	Tingogasta	-28.04	-67.34	1200
16.	87213	Chilecito Aero	-29.14	-67.26	945
17.	87217	La Rioja Aero	-29.23	-66.49	438
18.	87305	Jachal	-30.15	-68.45	1175
19.	87311	San Juan Aero	-31.34	-68.52	597
20.	87320	Chamical Aero	-30.22	-66.17	467
21.	87322	Chepes	-31.20	-66.36	658
22.	87328	Villa Dolores Aero	-31.57	-65.08	561
23.	87405	Uspallata	-32.36	-69.20	1890
24.	87412	San Carlos	-33.46	-69.02	940
25.	87416	San Martin	-33.05	-68.25	653
26.	**87418**	**Mendoza Aero**	**-32.50**	**-68.47**	**705**
27.	87436	San Luis Aero	-33.16	-66.21	710
28.	87448	Villa Reynolds Aero	-33.44	-65.23	485
29.	87506	Malargue Aero	-35.30	-69.35	1426
30.	87509	San Rafael Aero	-34.35	-68.24	745
31.	**87715**	**Neuquen Aero**	**-38.57**	**-68.08**	**270**
32.	87129	Santiago Del Estero Aero	-27.46	-64.18	198
33.	87222	Catamarca Aero	-28.36	-65.46	454
34.	87244	Villa De Maria Del Rio Seco	-29.54	-63.41	341
35.	87344	Cordoba Aero	-31.19	-64.13	484
36.	87349	Pilar Observatorio	-31.40	-63.53	338
37.	87453	Rio Cuarto Aero	-33.07	-64.14	420
38.	87532	General Pico Aero	-35.42	-63.45	139
39.	87623	Santa Rosa Aero	-36.34	-64.16	190
40.	87736	Rio Colorado	-39.01	-64.05	79

Table 2.3. Calculated RMS and bias scores for synoptic stations for HIRLAM simulations and ECMWF analysis for January 1998.

	HIRLAM		**ECMWF**		
	RMS	**bias**	**RMS**	**bias**	**No. of obs.**
2 m temperature (°C)	3.3	0.4	4.6	1.7	1579
2 m rel. Humidity (%)	14.7	1.5	20.8	3.8	1558
10 m wind speed (m/s)	2.8	-0.3	3.1	1.3	1590
m.s.l. pressure (hPa)	1.8	-0.2	1.9	-0.9	1315
cloud cover (octas)	3.3	1.6	3.1	0.5	1597

Table 2.4. Calculated RMS and bias scores for sounding stations for HIRLAM simulations and ECMWF analysis for January 1998.

	HIRLAM		**ECMWF**		
Wind speed (m/s)	**RMS**	**Bias**	**RMS**	**Bias**	**No. of obs.**
200 hPa	4.0	1.7	2.8	1.3	50
300 hPa	3.1	-0.1	2.1	0.4	50
500 hPa	2.7	-0.8	2.0	-0.3	48
700 hPa	1.9	0.5	1.7	-0.3	53
850 hPa	2.4	0.3	2.4	1.4	51
Temperature (°C)					
200 hPa	1.8	-1.4	1.5	-1.1	54
300 hPa	1.1	-0.6	0.8	-0.2	53
500 hPa	0.9	-0.5	0.9	-0.6	53
700 hPa	1.3	1.0	1.4	1.1	54
850 hPa	1.4	0.4	1.2	0.6	56
Relative humidity (%)					
200 hPa	13.3	-11.7	11.5	-10.2	35
300 hPa	13.3	-8.5	10.0	-5.8	43
500 hPa	9.7	-4.3	5.3	-0.9	46
700 hPa	11.3	-8.5	10.3	-8.5	32
850 hPa	11.9	-4.6	12.3	-5.1	40
Geopotential (m)					
200 hPa	17.1	-10.8	14.0	-7.1	52
300 hPa	11.1	0.9	8.4	-1.5	54
500 hPa	12.5	10.1	8.6	6.3	53
700 hPa	9.4	7.4	7.3	5.3	54
850 hPa	6.0	3.8	4.1	0.6	56

Four stations, which were judged to be representative for larger areas, were selected from the CENMA network. These are: Mallarauco (M16) which is located to the west, outside of the Santiago basin. La Platina (M01) which is located in an agricultural area south of Santiago. Entel (M07) which is located at the top of a tower in central Santiago and Lo Pinto (M04) which is located in the northern part of Santiago. Comparisons of observed and simulated time series of temperature at 2 meter and wind speed at 10 meter are shown in Figures 2.6 and 2.7. For wind direction at 10 meter (Figure 2.8) the average diurnal cycle is shown instead of a time series because the time series plot is difficult to read in this case. Below each figure the mean, standard deviation, maximum and minimum value is also given. It should be noted that the data from Entel is taken at the top of a 100 m high tower. For this location data from the lowest model level (~35 m) in HIRLAM is used for comparison.

A strong diurnal cycle is evident for both temperature and wind. The model simulations capture most of the variations in temperature at the four stations both on diurnal and longer time scales (Figure 2.6). The average values are within 1 °C for all stations except for Entel, which shows a cold bias during nighttime. This could be related to the fact that the data from the model is taken at a lower level than the observation. The simulated amplitude of the temperature is weaker than observed, in particular at Mallarauco. On the whole the agreement between model and observations for 2 meter temperature must be considered as good. Part of the difference in amplitude could be due to the fact that model output is at three-hour intervals while observed data is at one-hour intervals.

For wind speed (Figure 2.7) the differences between model simulations and observations are a bit larger than for temperature. The average difference is however less than or equal to 1 m/s. There is a strong diurnal variation of the wind speed which is captured in the simulation. For Mallarauco the simulated winds are higher than observed, especially during nighttime. At La Platina both the simulated average level and amplitude of the diurnal variation is very close to observed values. At both Entel and Lo Pinto the simulated wind speed during daytime is lower than observed. At Entel this can partly be explained by height of the station.

The observed wind direction (Figure 2.8) generally undergoes a diurnal variation with southerly or southwesterly winds during daytime and more easterly or southeasterly winds during nighttime. This variation is evident at Mallarauco, La Platina and Lo Pinto while the variation at Entel is less pronounced. The HIRLAM simulations generally show a weaker diurnal variation in the wind direction than observed. The difference in wind direction is largest during nighttime when the wind speeds are also low. This difference is probably due to small scale, topographically induced, circulations set up during nighttime which are not resolved by the HIRLAM simulation. During daytime the simulated wind direction is in better agreement with the observations.

At the synoptic station at Santiago airport; Pudahuel (to the west of Santiago, Figure 2.5 and Table 2.2) observations of additional parameters are available. Since this station is located close to Santiago a comparison of observed and simulated time series is shown also for this station. Figure 2.9 shows a comparison for cloud cover, wind speed and direction at 10 meter, temperature and relative humidity at 2 meter and mean sea level pressure. As for the other four stations the agreement for temperature is very good. The simulated wind speed is on average close to the observed but the amplitude of the diurnal variation is weaker than observed. The maximum wind speed during daytime is generally underestimated and the minimum during nighttime is overestimated. The variation in the

wind direction is also different than observed. As for the other four stations the wind direction is close to observed during daytime but not during nighttime. For this station the observed wind direction shifts to the north during nighttime probably as a result of the location of the station in relation to nearby mountains. The relative humidity shows a very strong diurnal variation both in the observations and in the model simulations. The amplitude and the mean values are similar in observations and model simulations. Cloud cover is a parameter that is more difficult to both model and observe accurately. The differences between model and observations are therefore largest for this parameter (c.f. Table 2.3). In January there is rather little cloudiness observed at Pudahuel. Cloud cover in excess of four octas (50%) is observed on 10 out 29 days, and in several of these cases for shorter periods than a day. HIRLAM predicts some cloudiness for most of the cases with observed cloudiness of more than four octas, but generally has a tendency to simulate less cloudiness than observed. On some occasions this can be linked to underestimated relative humidity, e.g. on the 15th and 20th.

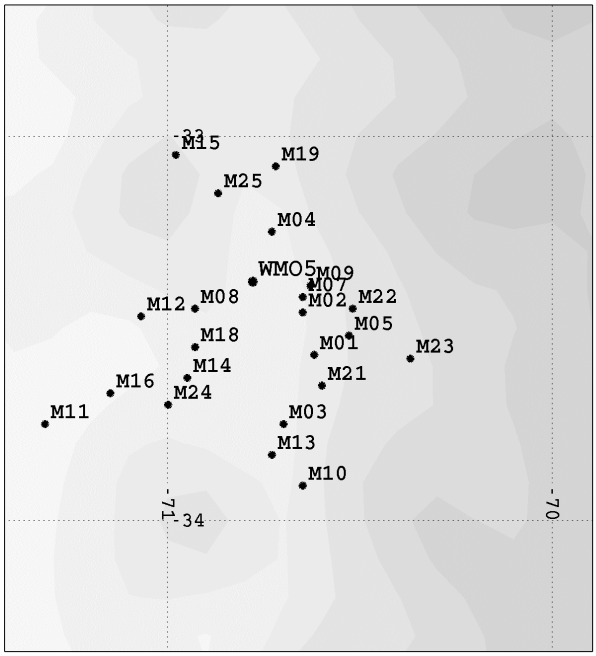

Figure 2.5. Map of the stations in the Santiago area, from Table 2.5. Pudahuel, (WMO-station number 5 in table 2.2) is also marked. The topography is the one used in HIRLAM.

Table 2.5. Stations in the Santiago area (Figure 2.5).

Stations	Name	Latitude	Longitude	Elevation (m)
M01	La Platina	-33.34	-70.37	652
M02	Esc.Ingeniería	-33.27	-70.39	534
M03	Los Tilos	-33.45	-70.42	486
M04	Lo Pinto	-33.15	-70.44	554
M05	Lo Cañas	-33.31	-70.32	643
M07	Entel	-33.26	-70.39	554
M08	Lo Prado	-33.27	-70.56	1065
M09	San Cristóbal	-33.24	-70.38	875
M10	Cuesta Chada	-33.55	-70.39	696
M11	Codigua	-33.45	-71.19	131
M12	María Pinto	-33.28	-71.04	180
M13	Paine	-33.50	-70.44	373
M14	La Campana	-33.38	-70.57	483
M15	La Dormida	-33.03	-70.59	1413
M16	Mallarauco	-33.34	-71.09	156
M18	Cuesta Barriga	-33.33	-70.56	883
M19	Quilapilún	-33.05	-70.43	615
M21	Pirque	-33.39	-70.36	676
M22	La Reina	-33.27	-70.31	680
M23	El Manzano	-33.35	-70.22	874
M24	El Paico	-33.42	-71.00	255
M25	Polpaico	-33.09	-70.52	520

2.4. Conclusions

A high resolution, dynamical, numerical weather prediction (NWP) model (HIRLAM) has been set up for an area covering part of Chile, including the area around Santiago. The purpose has been to provide meteorological input data for a regional atmospheric transport/chemistry/deposition model (MATCH). Using meteorological boundary conditions from ECMWF simulations have been performed with HIRLAM for the month of January 1998 producing a three-dimensional meteorological data set with three-hourly time resolution for the whole month. Comparison between model simulations and observations was made using data on wind, temperature, relative humidity, cloud cover and pressure at 32 synoptic, meteorological stations over the whole model domain. The comparison show that the HIRLAM simulation results in an improved description of the meteorological conditions near the surface of the earth compared to the analysis made at ECMWF for all parameters except for cloud cover. Comparison with observations from a dense network of meteorological stations in the region around Santiago show that the model simulations are able to capture a major part of the variability in temperature and wind speed in the region. The variations in the wind direction are more difficult to model accurately, especially during nighttime and for stations located close to small-scale topographic features. During daytime when the wind speeds are higher the agreement

between average observed and model simulated wind direction is good. For simulations of regional dispersion of air pollutants in the area of central Chile the meteorological data produced by the current set up of HIRLAM is judged to be sufficiently accurate. For detailed simulations of the dispersion of air pollutants in Santiago additional work is needed to include the influence of the city on the meteorological conditions, e.g. heat island and roughness effects. A higher horizontal resolution is also required to simulate small-scale topographic effects.

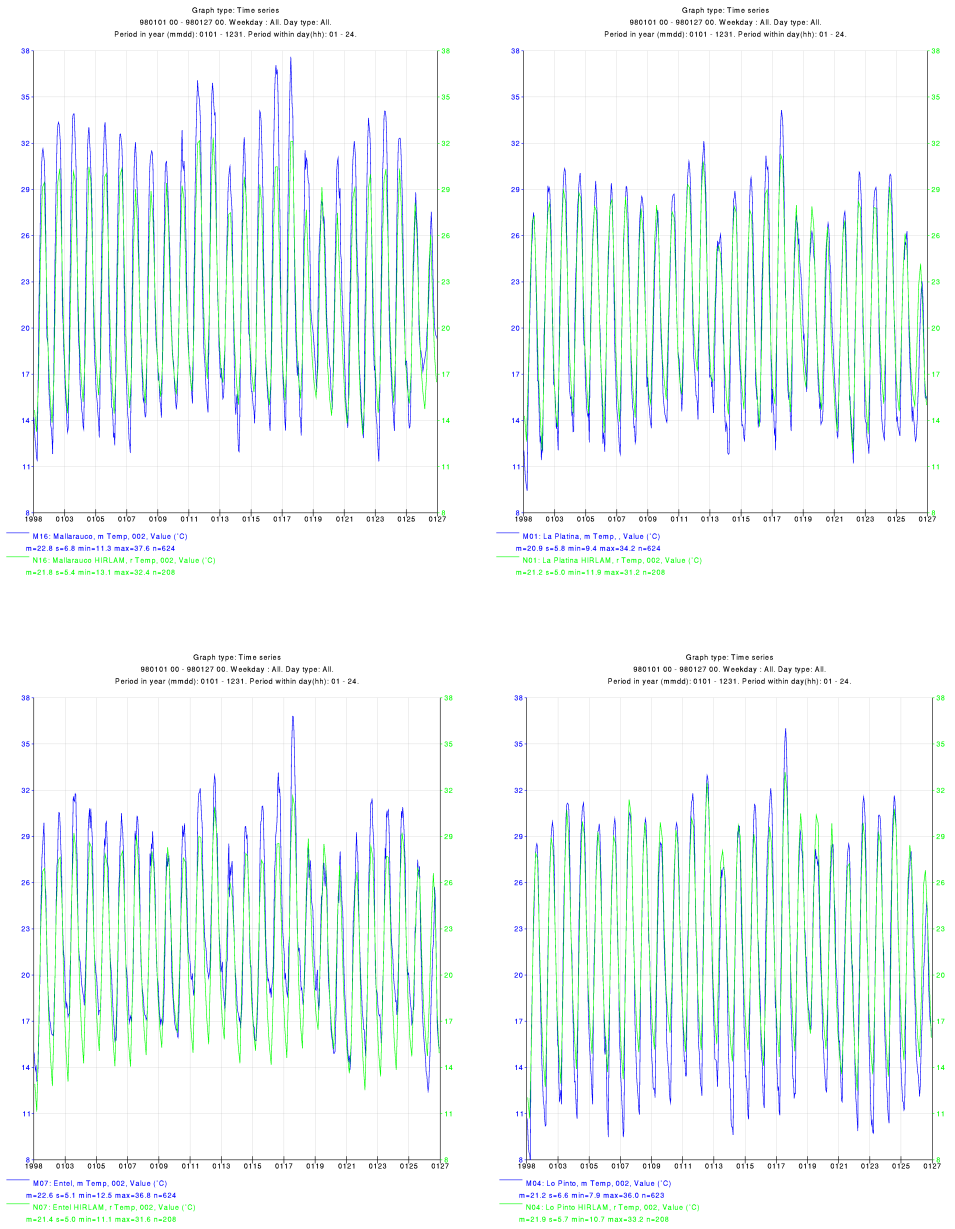

Figure 2.6. Model calculated (green) and observed (blue) temperature at two meter at the stations Mallarauco (M16), La Platina (M01), Entel (M07 100 m) and Lo Pinto (M04). Units: °C.

Figure 2.7. Model calculated (green) and observed (blue) wind speed at 10 meter at the stations Mallarauco (M16), La Platina (M01), Entel (M07 100 m) and Lo Pinto (M04). Units: m/s.

Figure 2.8. Model calculated (green) and observed (blue) wind direction at 10 meter at the stations Mallarauco (M16), La Platina (M01), Entel (M07 100 m) and Lo Pinto (M04). Units: deg.

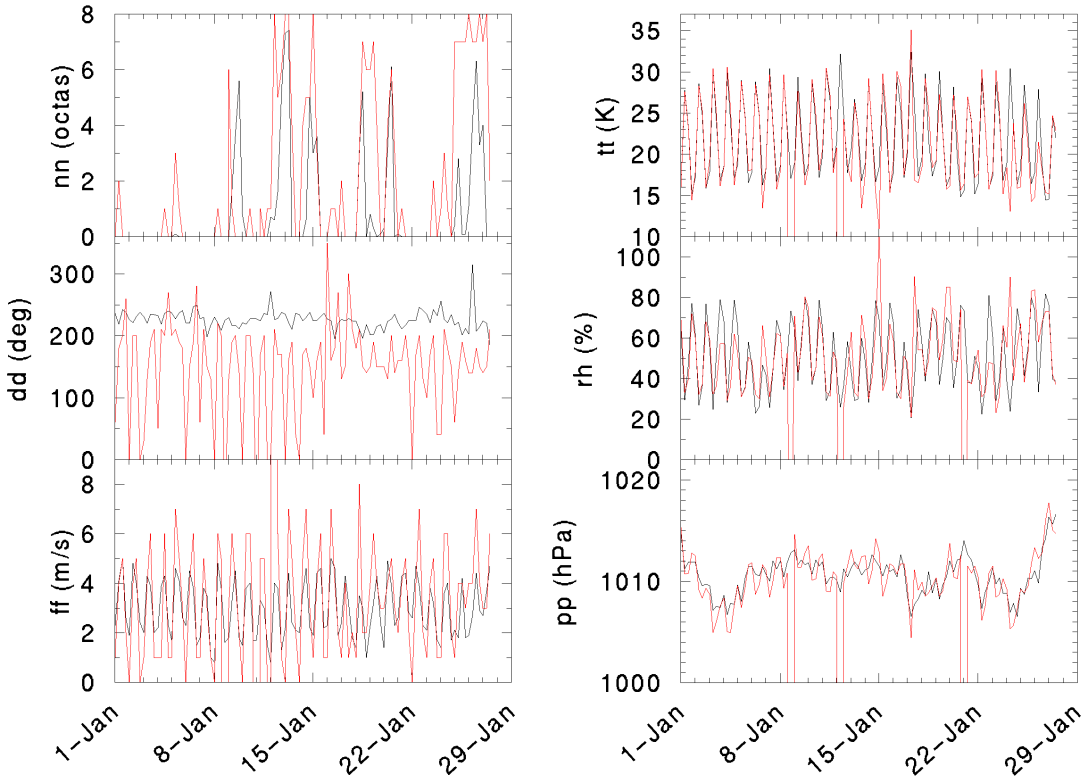

Figure 2.9. Time series of observed (red) and model simulated (black) cloud cover, wind direction, wind speed, 2 meter temperature, 2 meter relative humidity and surface pressure at Pudahuel (Table 2.2). Units: octas, degrees, m/s, °C, % and hPa respectively.

3. DISPERSION MODELING (MATCH)

L. Gallardo, G. Olivares and A. Aguayo
National Commission for the Environment, Chile

Urban and regional air pollution problems involve several spatial and temporal scales. The extension of such problems in the atmosphere range from tens to hundreds of kilometers in the horizontal, a few kilometers in the vertical and from a few hours to several days in time (e.g., Seinfeld and Pandis, 1998 and references therein). Therefore, local, meso-scale and synoptic transport patterns must be considered when assessing such problems. We assess the meteorological features of Central Chile through a meteorological limited area model called HIRLAM (See Section 2). Chemical and physical transformations occurring within these temporal and spatial scales must also be taken into account. This is done through a three-dimensional (3-D) tracer transport model that includes several chemical modules called Multi-Scale Atmospheric Transport and Chemistry Model (MATCH). MATCH is a limited area, off-line, Eulerian transport model developed at SMHI (Robertson et al. 1999, and references therein). The model adapts its horizontal and vertical resolution principally according to the input weather data. In this case, the model is run with a horizontal resolution of 0.05º latitude x 0.05º longitude (ca 5x5 km^2) and 15 levels in the vertical up to about 5-km.

As a first step, according to the availability of validation data, we focus on the chemistry of sulfur compounds. In this report, we describe a model application in which a simple sulfur scheme is used. This is a sulfur only scheme in which the oxidation of sulfur dioxide (SO_2) into sulfuric acid (H_2SO_4) and sulfate ($SO_4^{-2}{}_{(p)}$) is parameterized through a bulk reaction rate. In addition, as a complementary checking of the transport routines used in the model, we simulate the dispersion of carbon monoxide (CO) emitted mainly from urban sources in Santiago.

In the following pages, a brief description of the pollution problems that affect Central Chile is presented. Thereafter, we describe a first set of runs performed with the HIRLAM-MATCH system for Central Chile. Firstly, for assessing the performance of the transport routines in the model, we analyze the simulations of CO emitted from sources in Santiago. Further, we describe our oxidized sulfur simulations. All these modeling scenarios correspond to the HIRLAM simulations for January 1998 earlier described.

3.1. Problem description

The city of Santiago (33.5ºS, 70.8ºW) is located in a basin bounded by the high Andes (4500-m altitude on average). To the east, a lower parallel mountain range to the west (1500 m altitude on average), and two east-to-west mountain chains to the north and south of the basin respectively.

The climate of Central Chile is semiarid, largely controlled by radiative factors. The average rainfall in the Santiago area is about 300 mm per year, with large inter annual variability (Aceituno, 1988). The vertical exchange of air during most part of the year is controlled by the temperature inversion due to the subsiding branch of the Hadley cell. Prevailing winds in the basin are southwest winds throughout the year, although northwest winds also occur quite frequently during winter. The Mapocho and Maipo valleys provide some chimney-effect ventilation and cold-air drainage in the extreme phases of the daily

cycle. Altogether, the average meteorological conditions are unfavorable for the dispersion of air pollutants in the basin, especially during fall and winter. These stagnant anticyclonic conditions are further intensified in fall and winter by the presence of sub-synoptic features such as the coastal-lows, which bring down the base of the subsidence inversion (Rutllant and Garreaud, 1995). In spring and summer, the relatively larger insolation determines an increase in the depth of the mixed layer counteracting the accumulation of pollutants. Nonetheless, actinic fluxes are also increased during spring and summer accelerating the occurrence of a great deal of photochemical reactions.

Nearly one third of the population of Chile (i.e., about five million people) is found in the Metropolitan area of Santiago. This brings industries, private and public transportation, domestic and industrial energy consumption and other activities that result in large emissions of pollutants (See Table 3.1-1). On top of that, from other cities and some large point sources emanate other pollutants and pollutant precursors (e.g., Caletones and Ventanas copper smelters have annual emissions of sulfur dioxide of 0.38 TgS/yr and 0.06 TgS/yr, respectively).

Table 3.1-1 Emissions of particulate matter (PM), carbon monoxide (CO), reactive nitrogen oxides (NO_x), volatile organic compounds (VOC), and sulfur dioxide (SO_2) in Santiago. Unit: 10^3 tons per year. Source: CONAMA-RM, 1997.

Source	PM	CO	NO_x	VOC	SO_2
Stationary	3	4	11	1	17
Mobile	2	225	30	22	3
Other	37	16	3	39	1
Total	42	245	44	62	21

The combination of meteorological conditions adverse to the ventilation of the basin and of large emissions of pollutants to the atmosphere determines the occurrence of high concentrations of pollutants. Maximum concentrations of particles and pollutants associated with combustion process occur in fall and winter months, while in spring and summer there is a maximum in ozone concentrations. Lower concentrations of pollutants are observed in summer due to a better vertical mixing of the basin, although these concentrations frequently exceed Chilean and international air quality standards (CONAMA-RM, 1997).

Most of the available monitoring stations of air quality have been placed to assess, mainly, health effects due to air pollution in Santiago (See Figure 3.1-1). Nevertheless, it is very likely that significant concentrations of pollutants would be observed elsewhere in the basin if the monitoring stations were placed there. Several facts and considerations do indicate that this is the case. Firstly, due to their residence times in the atmosphere, fine particles (radii <10 μm), oxidized sulfur, hydrocarbons, ozone, etc., are all pollutants that can be regionally dispersed. High concentrations of these pollutants, particularly ozone, might have hazardous effects on vegetation and people's health (Crutzen, 1995 and references therein; García-Huidobro, 1999). Secondly, a haze layer can be readily observed throughout the year in the area and in other valleys than Santiago's. This type of haze may be associated with anthropogenic sources. Thirdly, short-term campaigns indicate the presence of anthropogenic aerosols outside metropolitan Santiago (Artaxo, 1998).

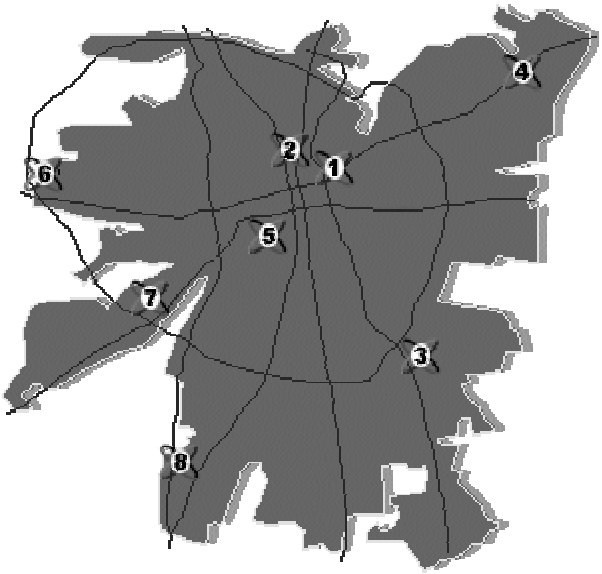

Figure 3.1-1. City of Santiago (33.5ºS, 70.8ºW) and location of the monitoring stations. For details See Table 3.3-1. Source: Servicio de Salud Metropolitano del Ambiente (SESMA).

3.2. Description and configuration of the modeling system

3.2.1. Model description

When describing a tracer's distribution, one has to take into account the movement of the air, the chemical transformations, the emissions and the deposition processes that take place. The way in which each of these processes is treated in HIRLAM-MATCH will be briefly described in the following sections.

a) Emissions

The basic version of the transport model MATCH includes modules for inclusion of area emissions of the simulated species. Emissions can be introduced at any vertical height in the model and at different heights simultaneously. The emissions are distributed in the vertical according to stability parameters using a simple Gaussian plume formulation as described by Robertson et al. (1996, 1999).

Information about emission rates within the model domain, about 200x400 km^2 around Santiago has been compiled. The most complete and up to date emission database is that of the Metropolitan area of Santiago managed through the "AIRVIRO" system (Törnvik, 1993) . The main source of information for other areas within the model domain than Santiago is the so-called "COSUDE" project. This is a cooperative program between Chile and Switzerland that aims a diagnostic analysis of air quality at five cities in Chile, among them Valparaíso (33º05'S, 71º40'W), Viña del Mar (33º01'S, 71º33'W) and Rancagua (34º10'S, 70º46'W). Within this project preliminary emission inventories have been performed (Jadrijevic et al, 1999).

The information about emission rates of sulfur dioxide and inhalable particulate matter from the large copper smelters in the area is rather complete because of the attainment plans have been established. Also, some industries have provided to CONAMA

information about their emissions for the formulation of several environmental standards (REF_As).

b) Transport

There is a large number (100 or more) advection algorithms that have been developed through the years, a fact that reflects the difficulties involved in the formulation of such schemes. The transport scheme utilized in MATCH corresponds to a generalization of the mass conservative schemes suggested by Bott (Bott, 1989). This procedure is computationally efficient and it reduces numerical diffusion. This scheme has been widely tested in several applications of MATCH and other tracer transport models (Langner et. al., 1998 and references therein).

Boundary layer processes, such as stability dependent dry deposition flux and turbulent vertical mixing in the boundary layer, are parameterized by means of the three primary parameters, surface friction velocity (u_*), surface sensible heat flux (H_0) and the boundary layer height (BLH). The horizontal diffusive fluxes are assumed small and neglected in the current set-up. Only the vertical turbulent mixing is accounted for. Transport by deep convection is not considered so far. A first order approximation of the turbulent flux intensity from mixing length theory is utilized. For details see Langner et. al. (1998) and references therein.

b) Chemistry

Three chemical schemes are included in the current version of MATCH:

- A sulfur only scheme in which the oxidation of sulfur dioxide (SO_2) into sulfuric acid (H_2SO_4) and sulfate ($SO_4^{-2}{}_{(p)}$) is parameterized through a bulk reaction rate
- A sulfur-nitrogen scheme in which the oxidation of SO_2 into H_2SO_4 and sulfate and of nitrogen oxides (NO_x=NO+NO_2) into nitric acid (HNO_3) and nitrate is represented. Also, the reactions between sulfuric and nitric acids and ammonia (NH_3) forming ammonium sulfate ($(NH_4)_2SO_4$) and ammonium bisulfate (NH_4HSO_4) and ammonium nitrate (NH_4NO_3) are modeled
- A complete photochemical scheme that model includes ca. 130 among 58 chemical compounds, including aromatics, ketones, peroxyacetyl nitrate (PAN), etc..

The sulfur only scheme is the one applied in these simulations. In this scheme there are two sulfur reservoirs: a SO_2 reservoir and a sulfate reservoir. The former represents SO_2 in gaseous phase and the latter gaseous H_2SO_4 and particulate sulfate ($SO_4^{-2}{}_{(p)}$). The overall model scheme is depicted in Figure 3.2-1. Notice that emissions of oxidized sulfur are assumed to occur in the form of SO_2 (95%) and of sulfate (5%). Dry and wet deposition parameters are included but described elsewhere. The oxidation of SO_2 is parameterized through a bulk reaction rate (KT) that involves both the gas phase oxidation through hydroxyl radical (OH) and through liquid phase reactions with ozone (O_3) and hydrogen peroxide (H_2O_2). The bulk reaction rate is based on an empirical expression proposed for Europe within the EMEP, i.e. European Monitoring and Evaluation Program (Tarrason and Iversen, 1998). The annual average of KT is modulated according to latitudinal, seasonal and diurnal variations. The maximum values are reached in the summer solstice whereas the minimum values are reached in the winter solstice. Additionally to the seasonal and

latitudinal variation, a diurnal variation is imposed to KT. The diurnal variation peaks at the local noon and it is a minimum at local midnight.

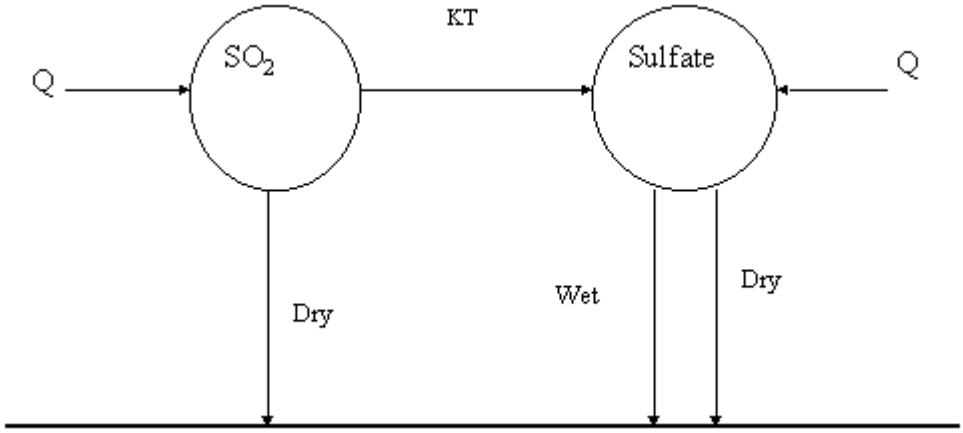

Figure 3.2-1 Linear sulfur scheme in MATCH. Q stands for emissions.

c) Deposition

The dry deposition process is modeled using a standard resistance approach. The deposition flux is proportional to the tracer's concentration and the inverse of the sum of the aerodynamic and surface resistance (Langner et. al., 1998). The different soil types are introduced in the surface resistance term. The loss due to wet deposition is parameterized in terms of a scavenging coefficient, which is different for each compound, and the precipitation at the surface (Robertson et al., 1996, 1999). The chosen parameters are shown in Table 3.4-1.

3.2.2. Model configuration

The set of tools provided by SMHI as part of this project allow the gathering and visualization of results and information about emissions, topography and meteorology for Central Chile. In Figure 3.2-2 a diagram of the system modules is presented.

AIRVIRO is the holder of the emission database, which is totally managed either by an internal module called EDB or by shell level commands,. i.e, through the user Interface provided by the operative system. AIRVIRO must be run on a Hewlett Packard workstation with Unix HP-UX O.S. and X-Windows installed. Also, AIRVIRO can display results provided by MATCH for each time step and height. This interface is under development by SMHI. In the mean time, we have used as a complementary visualizer GRADs, a freeware application capable of displaying GRIB files i.e, the compressed data format in which HIRLAM and MATCH outputs are presented. Tests are being performed with another freeware application (VIS5) available on the Internet.

MATCH is the dispersion model that receives through a script all the parameters that are needed to perform the modeling. The emission, topography and meteorology files must be in GRIB format. MATCH can be compiled and executed on almost any Unix platform with Ansi C and Fortran 77 compilers. SMHI is working on an integration of each module. Meanwhile, the AIRVIRO–MATCH modules communicate by means of independent applications that must by called manually on the shell.

MATCH reads HIRLAM outputs that are provided in GRIB format. HIRLAM is run on a supercomputer located in the Linköping University under the supervision and responsibility of SMHI. The HIRLAM outputs are then transferred to CONAMA over the net or on tapes.

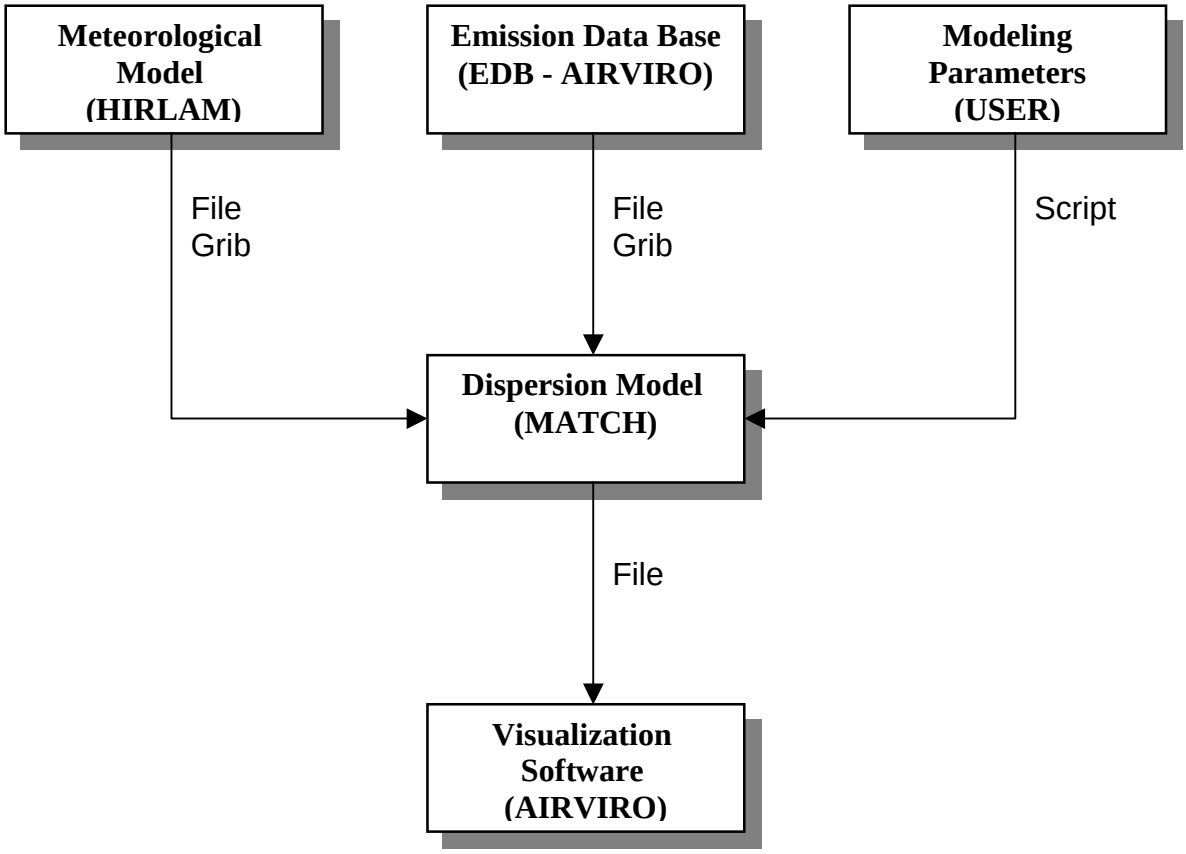

Figure 3.2-2. Diagram of the system modules for running HIRLAM-MATCH through the AIRVIRO interface

3.3. Simulations for a quasi-inert tracer

Like any transport tracer model, MATCH solves a continuity equation that calculates the changes in a tracer's concentration due to chemical and transport processes. Hence, to evaluate the model performance it is necessary to assess the performance of both the chemical and the transport routines. In the following pages, we show a description of the runs made for carbon monoxide (CO) with the HIRLAM-MATCH system for January. Given the data availability and the fact that CO has a relatively long tropospheric turnover time (Seinfeld and Pandis, 1998), we choose CO as transport tracer. In these simulations we consider the detailed emission inventories of CO available for Santiago for the 1997 scenario (CONAMA, 1997).

For validation, we use the data collected at the air quality network of Santiago. As stated before, this air quality network is designed to assess health effects derived from people's daily exposure to high concentrations of pollutants. Therefore, one has to be careful when comparing with model simulations, particularly on the regional scale. A regional model with a rather coarse resolution (5x5 km^2) cannot be expected to reproduce

local measurements that reflect local sources and human exposure to pollutants on short time scales (minutes to hours). The model is designed to reproduce the regional scale patterns of dispersion. Hence, our validation strategy for the air quality data in Santiago has its focus on comparisons with diurnal cycles and averages over longer time periods than one hour. Also, to avoid the effects of local sources and measuring conditions we compare with averages of several stations classified according to the observed variation and the emission patterns (See Table 3.3-1). We compare with the values calculated at the closest grid-box.

Table 3.3-1 Groups of monitoring stations according to observed variation and emission patterns for Santiago.

Sector	Monitoring stations
Central Santiago	Parque O´Higgins (33º27', 70º39'W)
Southern Santiago	La Florida (33º31'S, 70º34'W)
	El Bosque (33º32'S, 70º39'W)
Western Santiago	Pudahuel (33º26'S, 70º44'W)
	Cerrillos (33º29'S, 70º42'W)
Northern Santiago	Avenida La Paz (33º25'S, 70º38'W)
Eastern Santiago	Las Condes (33º22'S, 70º31'W)

3.3.1. Model set-up

The model was run with a horizontal resolution of 0.05ºx0.05º and 15 vertical levels. The domain corresponds to an area around Santiago of 200x400 km^2 and about 5.5 km in the vertical. Since CO behaves as an inert tracer, no chemistry was considered. Also, as the reported deposition velocities for CO are low (ca. 0.03 cm/s), the effects of deposition were neglected on the urban scale we look at.

A background level of 0.1 ppmv is prescribed all over the model domain. This value was chosen as representative of a global background according to literature (Kanakidou and Crutzen, 1999). As the CO emissions in the domain are large, the resulting mixing ratios in the model domain are dominated by the effect of the emissions and not by the background value.

3.3.2. Emission scenarios

The CO emissions over the domain are strongly controlled by the mobile sources. According to the emission inventory available for the Metropolitan Region (Santiago area), the total emissions are about 7500 gCO/s of which up to 96% correspond to mobile sources. In addition to the information available for Santiago, we include preliminary emission inventories for the cities of Rancagua, Valparaíso and Viña del Mar (Jadrijevic et

al,1999). However, since the emission inventory for Santiago is far more detailed and accurate than that available for other regions and up 99% of the total emissions in the model database are associated to sources in Santiago, we focus our analysis for Santiago. Probably, we underestimate the contribution of sources outside the Metropolitan Region. However, it is most likely that the CO concentrations in Santiago, where observation sites are located, are largely dominated by the sources in the area.

Two emission scenarios for CO were considered. These scenarios help us to determine which features can be reproduced by using a non-varying emission field, compared to those that can be assessed if more detailed information is available. This is important because in the case of sulfur, except at Santiago, only annual and monthly emissions are reported. Both scenarios are now described.

a) Annual average emission scenario

In this scenario, we apply a single emission field that is equal to the annual average emission for the domain (Cf. Figure 3.3-1). The emissions are put at 10-m and distributed in the vertical according to stability parameters using a simple Gaussian plume formulation as described by Robertson et al. (1996, 1999).

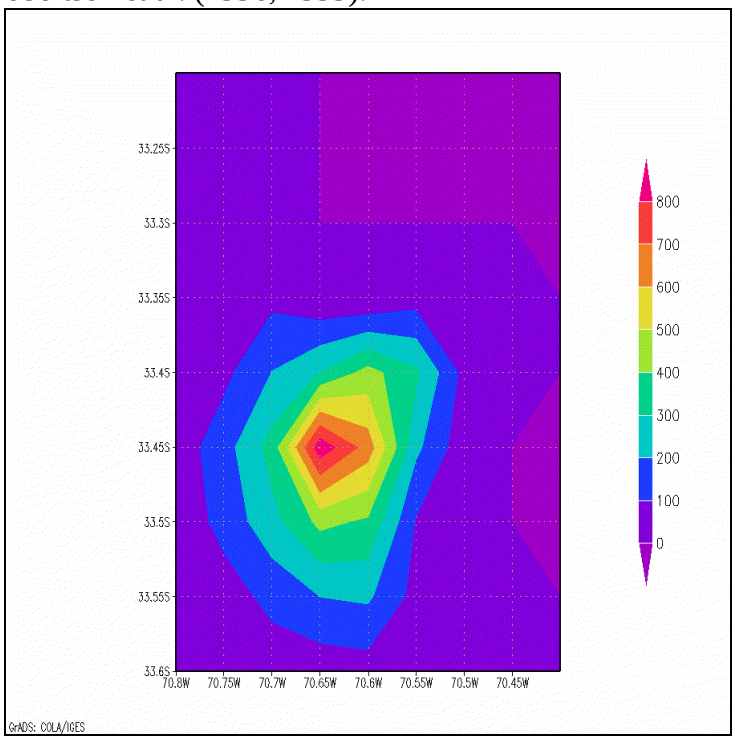

Figure 3.3-1. Spatial distribution of the CO emissions in gCO/s·km^2 over Santiago and surroundings (see color label for scale).

b) Hourly emission scenario

In this scenario, we apply emissions that are updated every hour during the simulations according to the information available in the emission AIRVIRO database. The emission inventory for Santiago has information about the diurnal, weekly and seasonal

variation of almost every stationary source in the area. In addition, for the street segments corresponding to mobile sources there is a diurnal, weekly and seasonal variation of the emissions. Again, the emissions are put at 10-m height and distributed in the vertical according to stability parameters.

The average emission cycle for Santiago is shown in Figure 3.3-2 for the first eight days of January. A strong diurnal variation, including the morning and evening rush hours can be seen. Also, there is a weekly cycle with lower emissions during the weekend than in the weekdays. These features vary inside Santiago, as is shown in Figure 3.3-3. In Central Santiago the emission cycle is similar to the average, while in Eastern Santiago there is a midday maximum and almost no weekly variation (Cf.figure 3.3-4)

The emission rates do also depend on the location. Central Santiago shows the largest CO emissions in the model domain whereas Eastern Santiago shows the lowest emission rates, ca. two orders of magnitude lower than those do in Central Santiago. Notice that at most locations the morning maximum is sharper than the evening maximum.

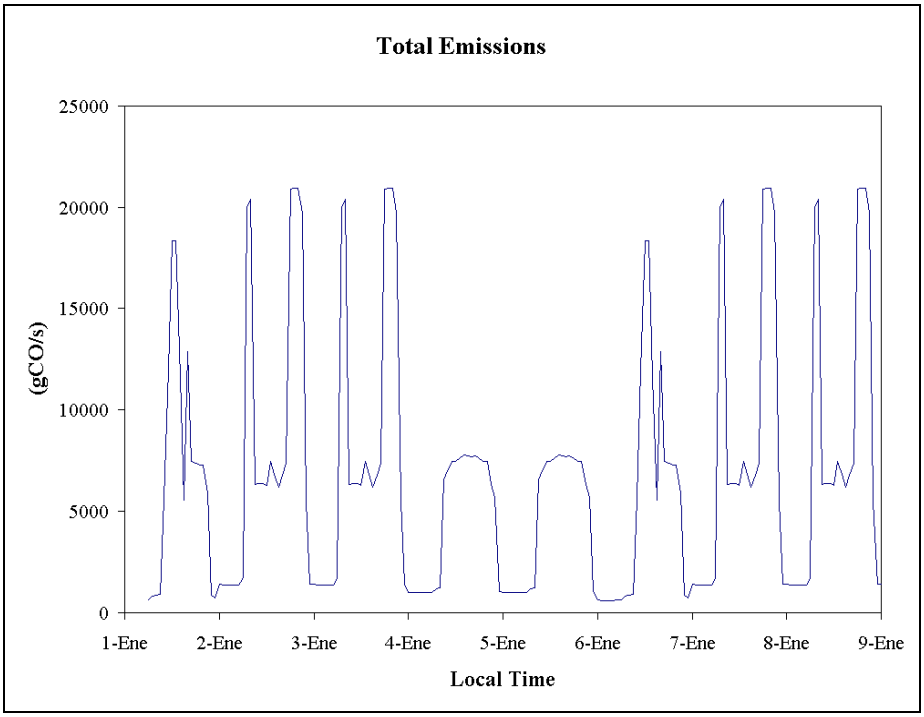

Figure 3.3-2. Santiago average emission variation.

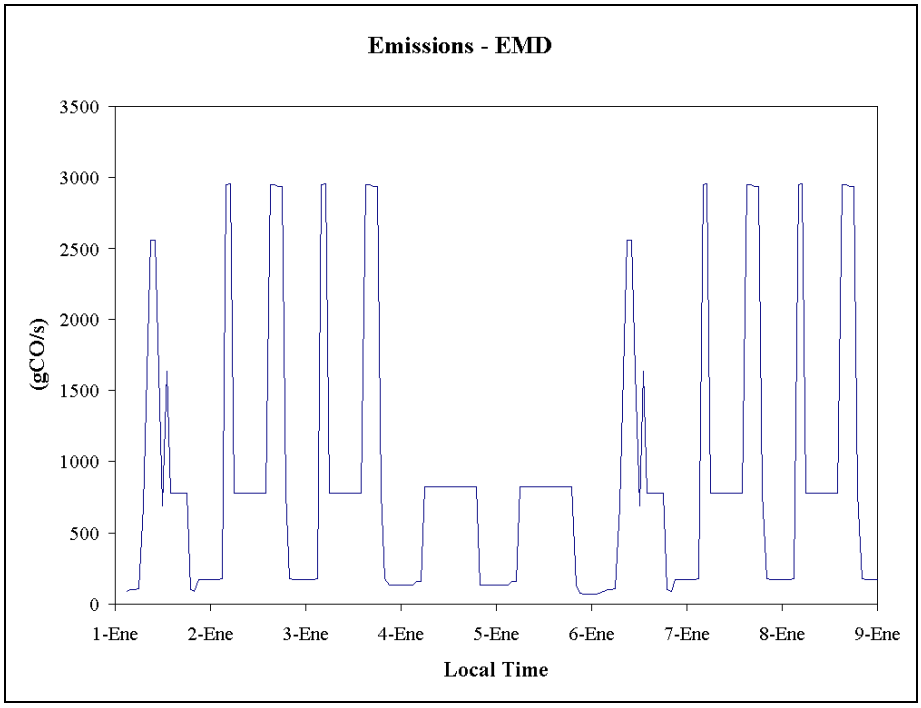

Figure 3.3-3. Central Santiago emission variation.

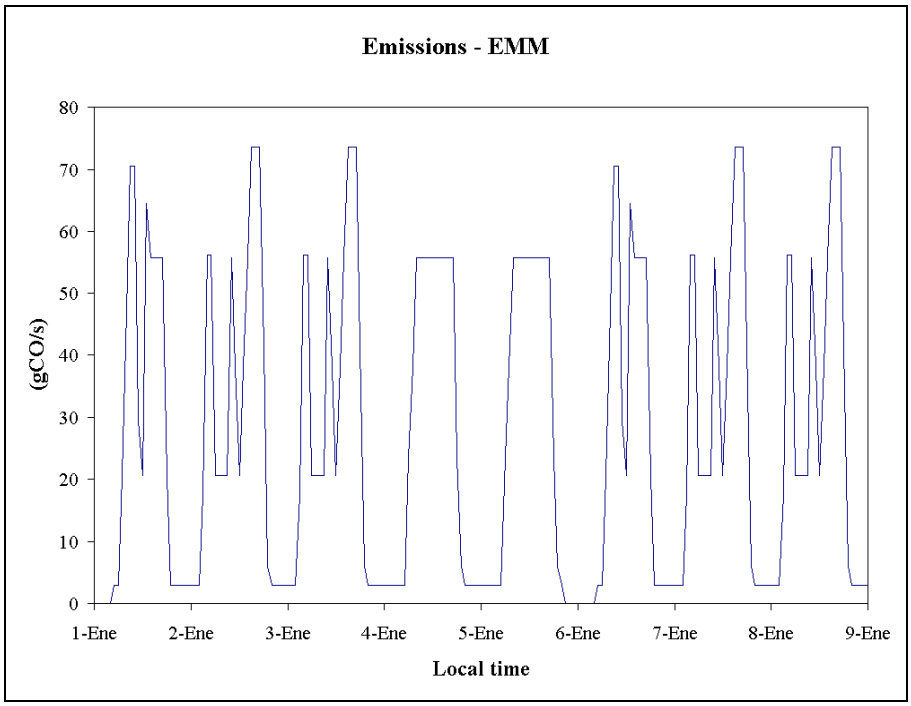

Figure 3.3-4. Eastern Santiago emission variation

3.3.3. Results and validation

The CO distribution estimated by the model for the January 1998 with the hourly emission scenario captures the major characteristics of the distribution actually observed (See Figure 3.3-5). The maximum concentrations occur in Central Santiago where the largest emissions take place (Cf. Figure 3.3-1). North-south and east-west gradients also appear. The annual average emission scenario also captures these characteristics.

The model is able to capture the overall diurnal variation with highest concentrations in the morning and evening rush hours (Cf Figure 3.3-6). However, the daytime concentrations tend to be overestimated and the nighttime values underestimated. During the afternoon a lowering of the concentrations occur in connection with the intensive vertical mixing and the ventilation driven by the sun's heating, typical of summer conditions.

Since the atmosphere is typically stable in the early morning, the morning maximum in CO is dominated by the local emissions. In fact, the monitoring stations in Santiago show a rather sharp maximum in CO concentrations between 7 and 8 AM that coincides with the rush-hour emissions. In the evening, a much broader maximum is observed.

When looking in more detail at different sectors in Santiago, the impact of local sources and the changes in meteorological conditions at different areas of Santiago become apparent. Figure 3.3-7 shows the analogous comparison shown in Figure 3.3-6 but for each of the sectors defined in Table 3.3-1. As stated before, the model is generally able to reproduce the diurnal variation that follows from the variation of the CO emission, mainly related to transportation. However, the daytime values are typically well captured whereas nighttime values tend to be underestimated.

Similarly to other stations, the diurnal cycle at Central Santiago is reproduced by the model, however there is a tendency to overestimate the daytime concentrations. This may be related to the lack of an appropriate description of the soil type in the area. The model assumes so far a rural surface free of vegetation, whereas in reality Central Santiago is covered by buildings and pavement that produce a noticeable heat island effect. The boundary layer height at the grid-box representative for Central Santiago is shown in Figure 3.3-8. Notice that the maximum in BLH occurs at 15 hours, coinciding with the strongest insolation. Also, synoptical variations are observed in the data series shown in Figure 3.3-8. We cannot assess how realistic these values are as the only vertical sounding available for Santiago at La Platina (70º37' W, 33º34'S, 652 m.a.s.l) reported rather fragmentary and unreliable data for January 1998. We expect to improve the BLH calculations through the inclusion of a better soil type data that we have recently received and that will allow a better representation of the heat island effect produced by the city. In addition, the sounding data is more reliable later in 1998 and 1999.

Other concurrent explanations for the model's tendency to overestimate daytime concentrations at Parque O'Higgins are related to inaccuracies of the emission inventories themselves or problems derived from the interpolation procedures applied for obtaining the gridded emission files required by MATCH. The grid-box representative for this station has a strong emission (3000 gCO/s) partially associated with a highway that crosses Santiago in the north-south direction (Avenida Norte-Sur). The monitoring station is placed several hundred meters from the highway and a small hill covered by relatively high (ca 10m) trees separates the highway from the monitoring station. Thus, the model may be overestimating

the emissions for the grid-box and the monitoring station may not be capturing all of the impact from the highway.

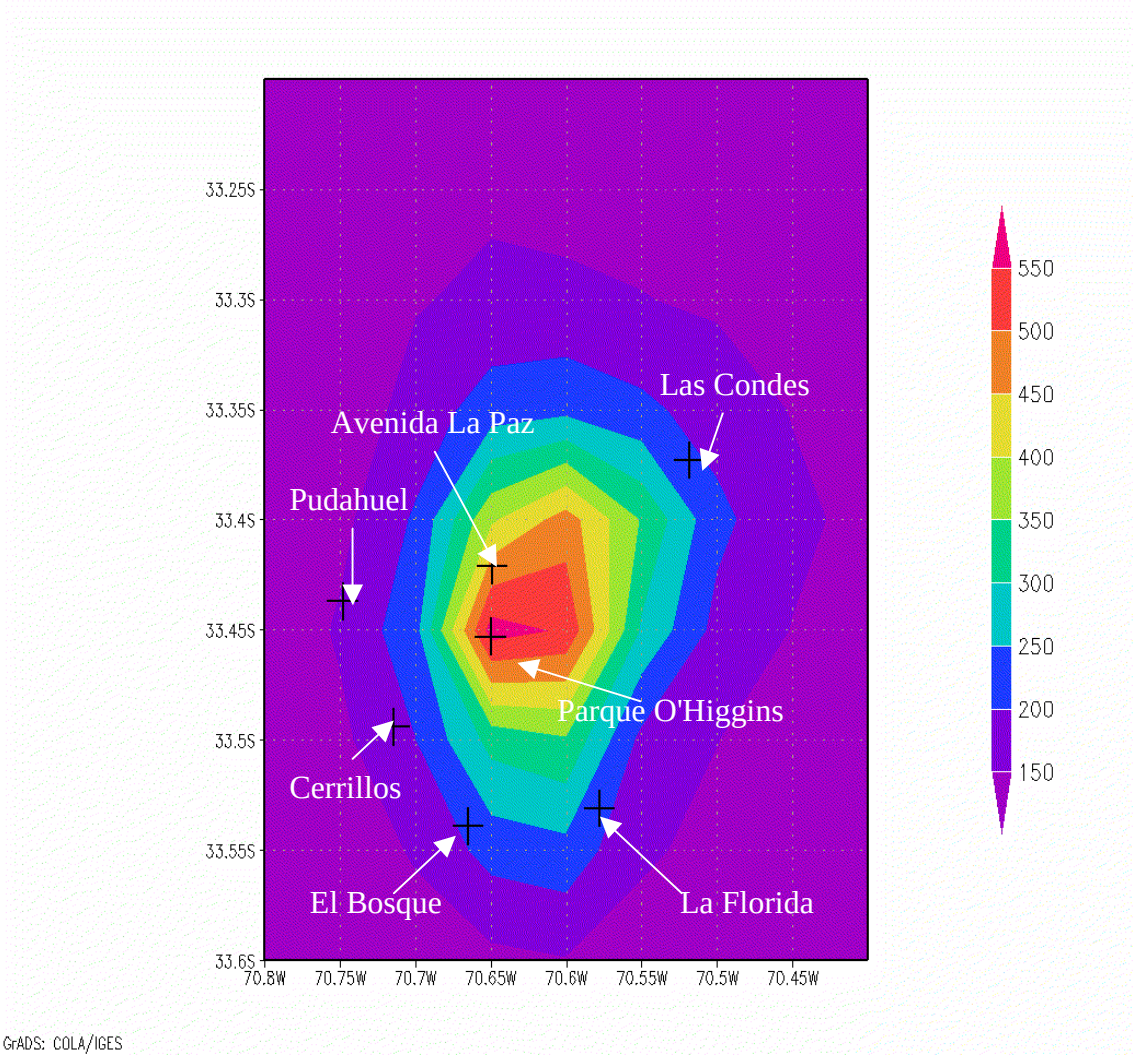

Figure 3.3-5. Monthly mean distribution of CO at surface (10 m) in the Santiago area as calculated by the model. The crosses indicate the location of the stations of the air quality net in Santiago. Units, mgCO/m^3.

Next we attempt to assess a mechanism that has been suggested for explaining the high concentrations of pollutants in western and southern Santiago. This mechanism is related to the air movements caused by the up and down-slope winds driven by radiation. Accordingly with the prevailing winds, during daytime the large primary emissions of pollutants that take place in Central Santiago are transported towards and accumulated in Eastern Santiago. During night, when the winds turn to down-slope winds, the pollutants are transported westwards. The model shows in fact such a behavior for CO. This is illustrated in Figure 3.3-9 where average cross sections in east-west direction over Santiago are shown. Nevertheless, the model tends to underestimate the nighttime concentrations, particularly in Southern Santiago. This could be due to an exaggerated layering of the lowest model levels that reduces the chances for downward mixing of CO. In fact, during night the BLH falls down to 150 m that is the minimum BLH prescribed in the model.

However, local sources, which the inventory does not account for, cannot be ruled out. Particularly in Southern Santiago, where the observations show a midnight maximum that is only 20% lower than the morning maximum associated with transportation.

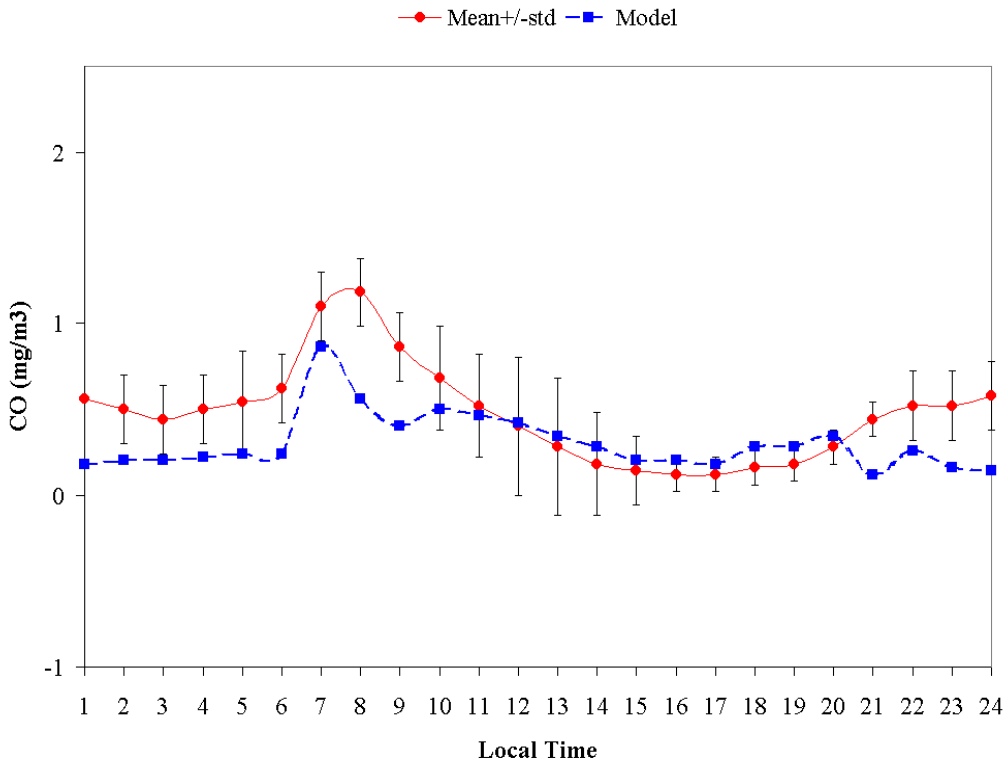

Figure 3.3-6. Average diurnal variation of CO concentrations in Santiago during January 1998 according to observations and model simulations. The circles indicate observations and the squares simulated values. Error bars indicate one standard deviation of the mean.

In Eastern Santiago the model simulates the advection of CO from the large emissions that take mainly place in Central Santiago, which are two orders of magnitude larger than those in Eastern Santiago. This advection effect explains the concentrations observed in the afternoon consistently with the prevailing winds. However, the bimodal peak of morning and noon hours is not well simulated. The local sources of CO show a diurnal variation consistent with the observations, however according to the simulations the impact of local sources in this part of the city is negligeble compared to the advection effect. This may be associated with an underestimate of the emission rates, however other biases cannot be ruled out. One such a bias could be due to the rather rough topography and roughness data we use, which may result in unrealistic winds and vertical mixing at some places (Cf. Section 2).

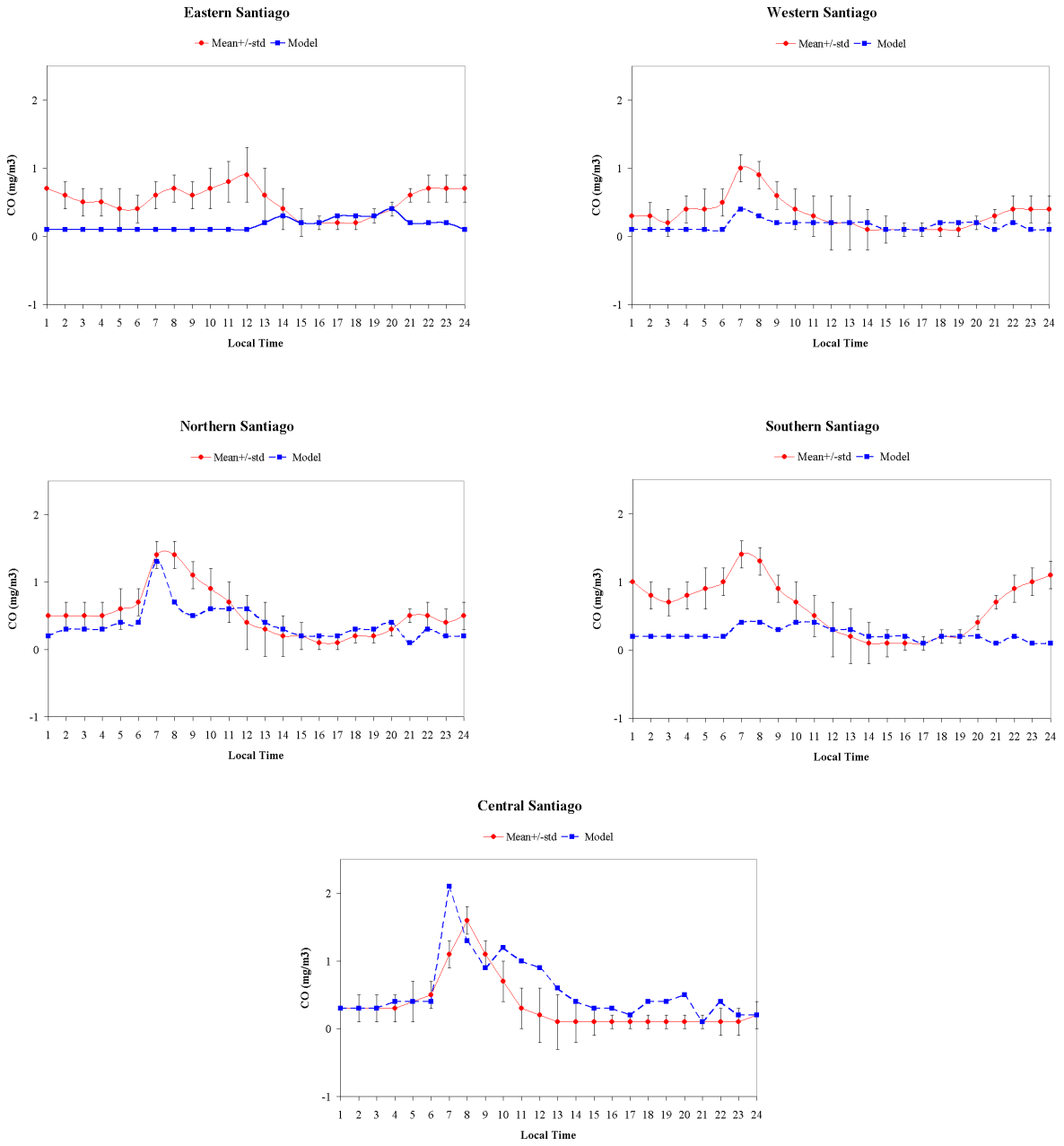

Figure 3.3-7. Local comparison by sectors. The circles indicate observations (every hour) and the squares simulated values (every three hours). Error bars indicate one standard deviation of the mean.

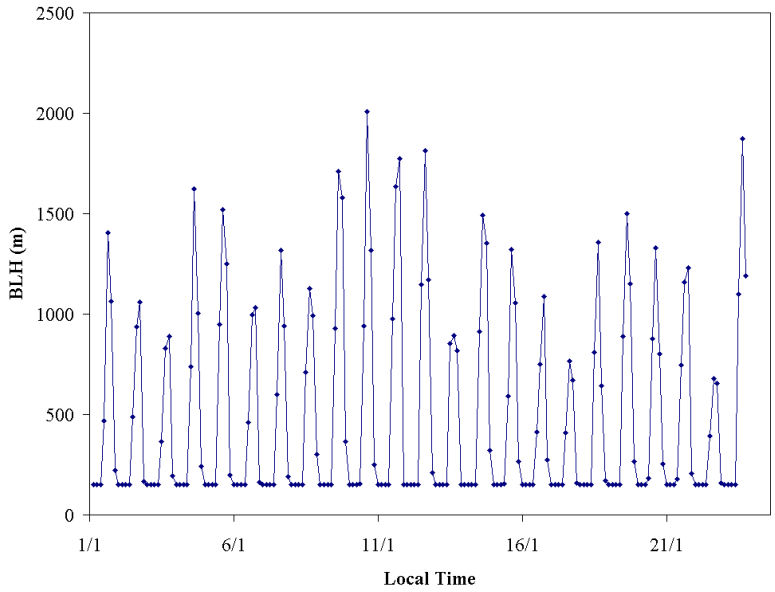

Figure 3.3-8. Boundary layer height at the grid-box for Parque O'Higgins.

3.3.4. Summary

Runs for CO were made to evaluate the performance of the transport module of the MATCH model. Two emission scenarios were considered in the runs. One in which an average emission rate is applied and another in which emissions are allowed to vary on an hourly basis. Both scenarios capture the major characteristics of the horizontal distribution of CO in Santiago. A diurnal cycle with maximum concentrations in connection with morning and evening rush hours are apparent from both the observations and the model simulations. However, the model tends to overestimate the daytime concentrations and to underestimate the nighttime concentrations. The former is probably related to the fact that in these simulations the model does not account for the heat island effect caused by the urban area. The latter may be related to shortcomings in the emission inventory. However, shortcomings related to the land-use data applied so far cannot be ruled out. The model simulates perhaps too strong a stability in the boundary layer during nighttime that inhibits the vertical mixing of CO from aloft. Nevertheless, the model simulates a recycling of CO within the basin associated with the radiation driven circulation.

In sum, the model is able to reproduce the regional patterns of dispersion and a rather accurate picture can be obtained by applying average emission scenarios. However, a more detailed emission inventory is required for assessing local effects. Furthermore, detailed land-use data must be incorporated in order to better simulate vertical mixing processes in the boundary layer.

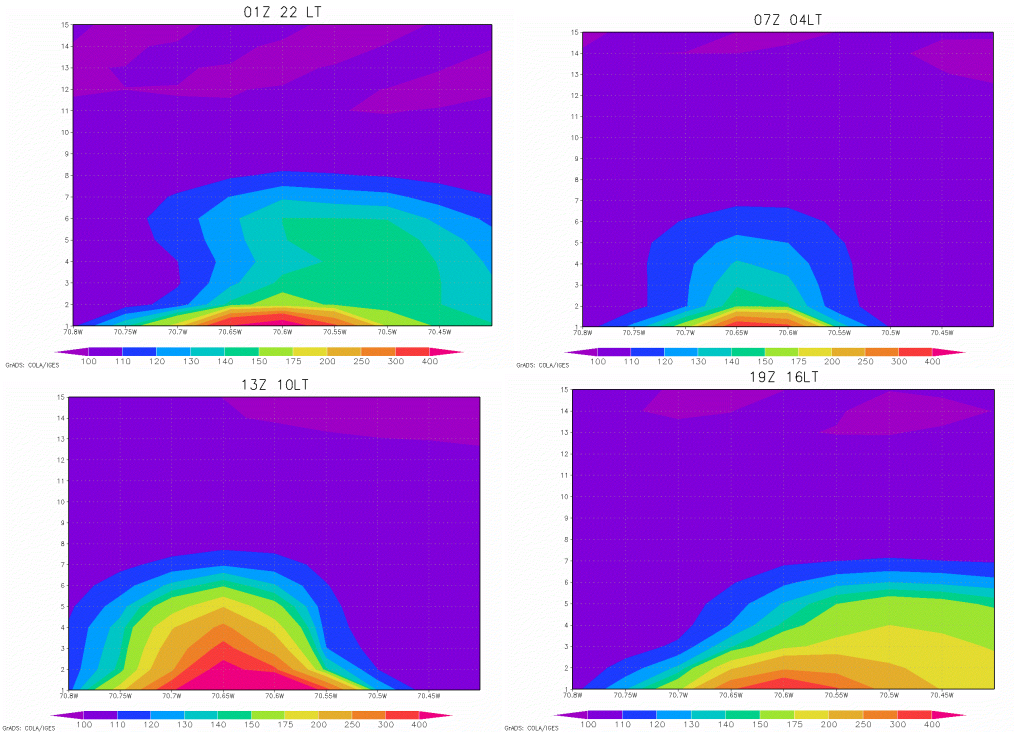

Figure 3.3-9. Average cross sections in east-west direction over Santiago for CO (ppmv) in the period January 1-23 as simulated by the model. From top-left clockwise, the corresponding local time is 22:00, 04:00, 16:00, 10:00.

3.4. Simulations for oxidized sulfur

3.4.1. Model Set Up

The model is run for the same configuration as that shown for CO, except for the chemistry and deposition modules. The chemical scheme used in these runs is the linear sulfur scheme earlier described. The deposition velocities adopted are presented in Table 3.4-1.

Table 3.4-1 Dry deposition velocities for SO_2 and sulfate to different surfaces (cm/s) and wet scavenging coefficients ($s^{-1}\cdot(mm\cdot hour^{-1})^{-1}$).(Langner et. al., 1998)

Component	Dry Deposition			Wet Deposition
	rural day	Rural night	sea	Scavenging coefficient
SO_2	0.8	0.3	0.80	$6.95\cdot10^{-5}$
SO_4	0.1	0.1	0.05	$2.78\cdot10^{-4}$

The background values of SO_2 and sulfate were assumed to be zero. We are not aware of any background measurements of oxidized sulfur in Central Chile to support our

assumption. However, available measurements indicate a rapid decay of the concentrations off the emission sources. Moreover, since the SO_2 emissions within the domain are very large it appears not to be unreasonable to neglect the background of oxidized sulfur. A larger bias associated with natural sources of sulfur may be found in coastal areas. Nevertheless, there are large SO_2 sources in those areas too.

3.4.2. Emission scenarios

One of the objectives of this project is to assess the relative contribution of different sources to the overall air pollution problem in the region. At this stage, we focus on the relative contributions of urban sources in Santiago and the copper smelters in the area. The emissions scenarios considered were:

- ***Santiago emissions***: This scenario groups all the sources identified in the Santiago emission inventory for 1997, excluding the cement plant of Polpaico, located to the northern part of the city. This emission scenario includes all the information available for the Santiago sources in terms of their diurnal, weekly and monthly cycles. This scenario groups ca 3% of the total emission (15 kg SO_2/s).
- ***Regional emissions***: This scenario corresponds to all the emissions outside Santiago, excluding the copper smelters. This scenario considers only an average field since there is no information about the emission cycles in other cities than Santiago. This scenario groups 1% of the total emission.
- ***Megasources***: Here all the megasources within the domain are considered, the copper smelters (Caletones, Chagres, Ventanas) and the Polpaico cement plant. These emissions are located at different heights. The copper smelters were placed in the model at 300 m whereas Polpaico at 50 m. This scenario sums up to 96% of the total emission of SO_2.

3.4.3. Results and validation

The oxidized sulfur distribution over Central Chile is largely dominated by the copper smelters located in the area (Cf. Figure 3.4-1). This is not surprising because of the size of the emissions associated to such industries and because of the characteristics of sulfur. The smelter's emissions of oxidized sulfur sum up to 95% of the total emissions in the area. These emissions of mainly sulfur dioxide are regionally dispersed according to the prevailing weather patterns and to the turnover time of the species.

The predominance of the copper sources occurs both in horizontal and vertical distributions (Cf. Figure 3.4-1 and Figures 3.4-2). The urban emissions have a modest impact, i.e., less than 10%, layer on the sulfur burden outside the urban areas, and above the mixed in comparison with the copper smelters. Moreover, as discussed later, at some occasions the smelters contribute significantly to the sulfur burden in the urban areas in connection with strong vertical mixing.

Regarding the partitioning between SO_2 and sulfate, little can be said at this stage. The simulated partitioning is shifted towards the SO_2 reservoir, however this is a preliminary result and it must be carefully checked in the up-coming simulations. On one hand, the oxidation rate could be overestimated as it is calibrated for observations in Northern Europe where aqueous face reactions are probably much more important than over Central Chile in summer. On the other hand, the effects of heterogeneous reactions are

not considered which may lead to an underestimate of the oxidation rate. Unfortunately, to the best of our knowledge no measurements of sulfate are available for the period under consideration to help us to assess the actual partitioning between SO_2 and sulfate. However, campaign measurements of sulfur species and other relevant parameters will soon be reported for winter and spring conditions of 1999 (Oyola, pers. communication). Also, some indications of the actual partitioning are reported for winter conditions (Artaxo, 1998). These data together with an explicit and separate treatment of gas-phase and aqueous-phase oxidation processes in the model will allow us to better assess this issue in the next months.

In the following, we compare the model results against available observations in Santiago, at Talagante and at some stations outside the Metropolitan area of Santiago.

a) Santiago and Talagante

The observed diurnal variation of the SO_2 concentrations over Santiago shows two maxima (See Figure 3.4-3). A first maximum occurs regularly at ca. 8 AM. A second one occurs at ca. 2 PM. The morning maximum appears to be associated with urban emissions, probably transportation as it coincides in time with the morning maximum discussed for CO. Moreover, the spatial distribution with a stronger maximum in the western and southern parts of Santiago indicates that this morning maximum is associated with transportation sources, mainly those that use diesel (Cf. Figure 3.4-3). The afternoon maximum occurs at all stations on an episodic basis. This episodic character can also be seen from the larger dispersion of the data during the afternoon than the rest of the day.

During January 1998, several afternoon maxima in SO_2 concentrations were observed at all Santiago stations and at Talagante (33º37' S, 70º51' W), a semi-rural station west from Santiago (not shown here). The ubiquous appearance of these afternoon maxima suggests that it reflects a long-range transport, probably associated with the large-copper smelters outside the Santiago basin. It must pointed out that these events appear earlier in the west than in the east following the maximum in insolation. The occurrence in connection with the strongest insolation suggests that the episodic afternoon-maxima are linked with vertical mixing processes that may bring sulfur from aloft (fumigation).

The model captures the morning maximum due to urban sources for monitoring stations in Santiago (Cf. Figure 3.4-4). Again, the temporal and spatial distributions simulated by the model suggest that this source is associated with transportation. At Talagante, if any the morning maximum is much smaller than that in the afternoon (not shown here). The latter, as for the Santiago stations, appears at the hours of strongest insolation when the thermally driven vertical mixing is strongest.

The different effects of Santiago surface sources and the megasources are further illustrated by the observations and simulations for the monitoring station at Talagante on January 17 1998. On that date, an afternoon maximum in SO_2 is observed at Talagante, reaching up to 22 $\mu g/m^2$. According to the model simulation, a plume of SO_2 was effectively advected from the southeast over the Santiago basin during January 17. This is illustrated in Figure 3.4-5, which shows the 24-hours average of the horizontal distribution of SO_2 integrated in the vertical.

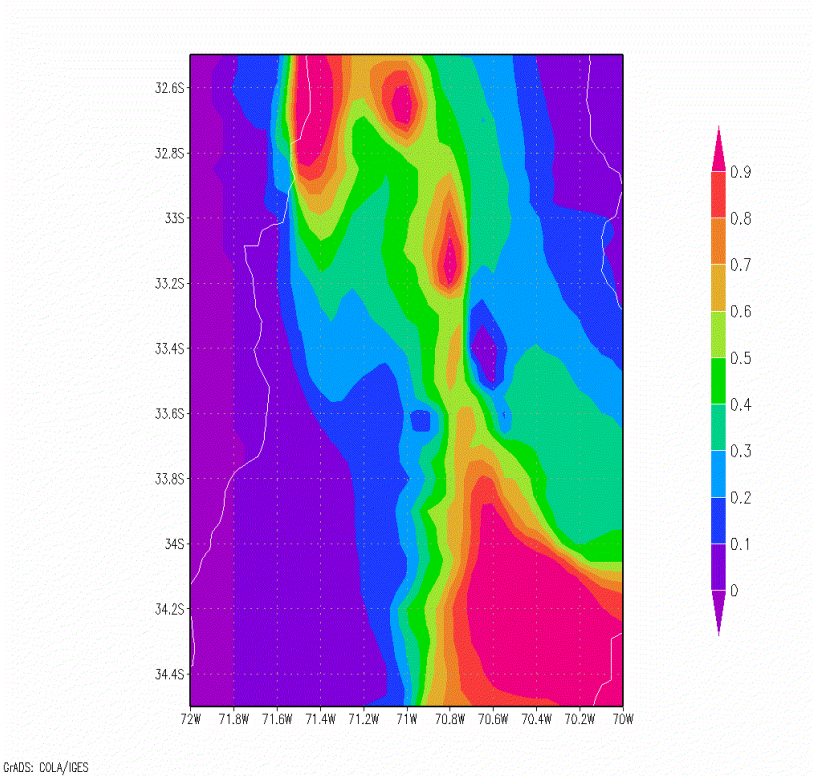

Figure 3.4-1. Average relative contributions of smelters to the oxidized sulfur burden (SO_2 plus sulfate) at surface. The contribution is expressed in fraction of the total concentration, for the period January 1 to 23.

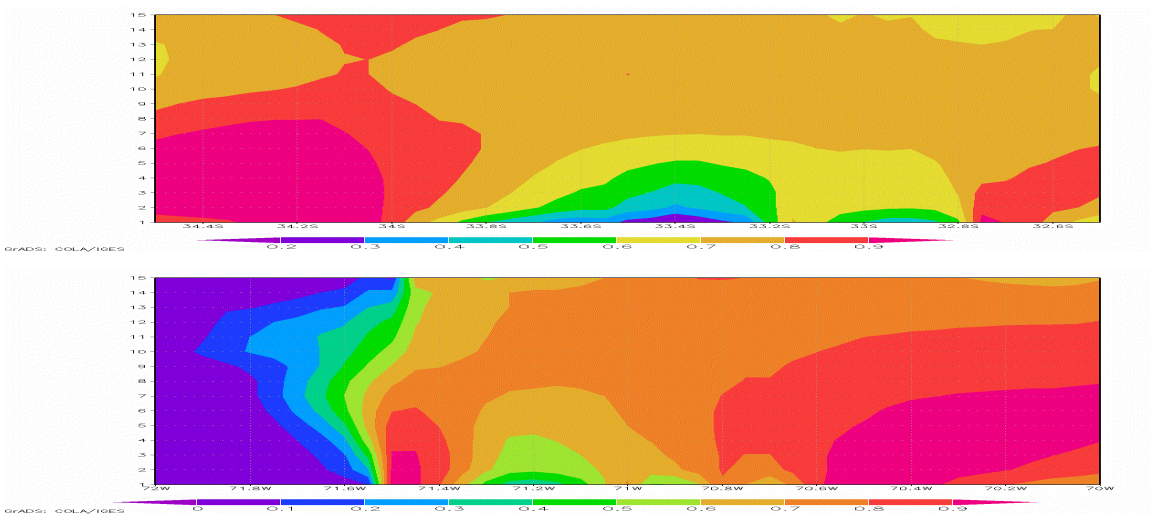

Figure 3.4-2. Vertical cross sections (N-S upper panel and E-W lower panel) average relative contributions of smelters to the oxidized sulfur burden (SO_2 plus sulfate). The contribution is expressed in fraction of the total, for the period January 1 to 23.

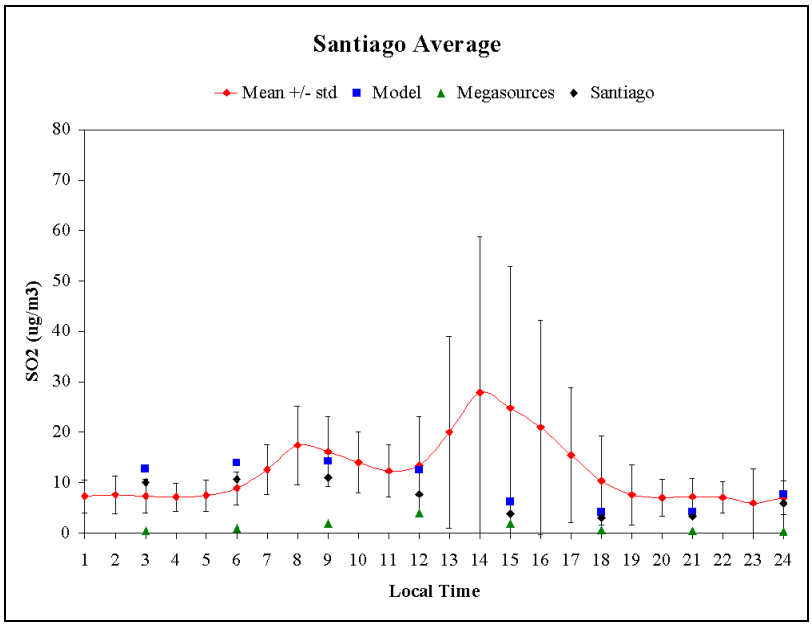

Figure 3.4-3. Average SO_2 concentrations as observed by monitoring stations in Santiago for January 1998 (line and circles) and as simulated (squares).

The average effect shown in Figure 3.4-5 does, of course, vary along the day. Figure 3.4-6 shows a sequence of north-to-south cross-sections of the SO_2 distribution averaged over the model domain (east-west). Notice that only during daytime and particularly in the afternoon, the plumes from the copper smelters are mixed down from aloft resembling a fumigation process on a regional-scale.

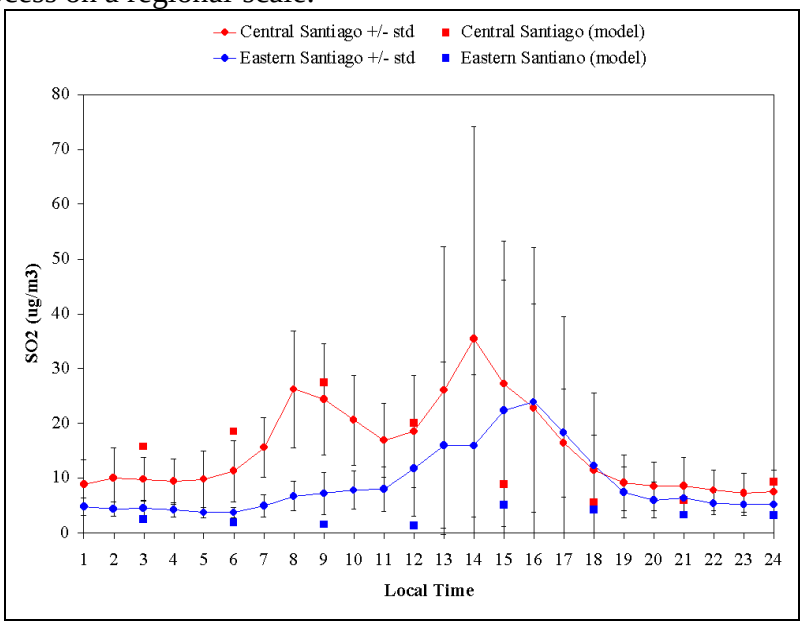

Figure 3.4-4. SO_2 concentrations at two different areas of Santiago. The observations are represented by circles and the simulations by squares.

The early afternoon maximum in SO_2 concentrations observed at Talagante on January 17 is captured by the model even on an hourly basis, however the calculated

maximum SO_2 appears some three hours earlier than in the observations (See Figure 3.4-7). This shifting may be related to shortcomings in the boundary layer parameterization in nighttime and early morning. During night and in the early morning, until 8 AM local time, the boundary layer height in the model falls to 150 m that is the minimum value prescribed. At those hours, local sources dominate the calculated SO_2 concentration at Talagante. The impact of long-range transport (smelters) takes place later by 9-10 hours, when the sun goes up and the boundary layer grows. The increased vertical mixing allows the transport of SO_2-rich air from upper model layers, where the smelters dominate the SO_2 content. This results in an increase of the surface concentrations. Later by 13 hours, despite the downward mixing of SO_2-rich air, the model estimates lower SO_2 concentrations than in the morning hours as it reaches the strongest vertical mixing and the deepest mixing layer. We expect to improve these simulations as the soil information is improved allowing a better representation of latent and sensible heat fluxes in nighttime.

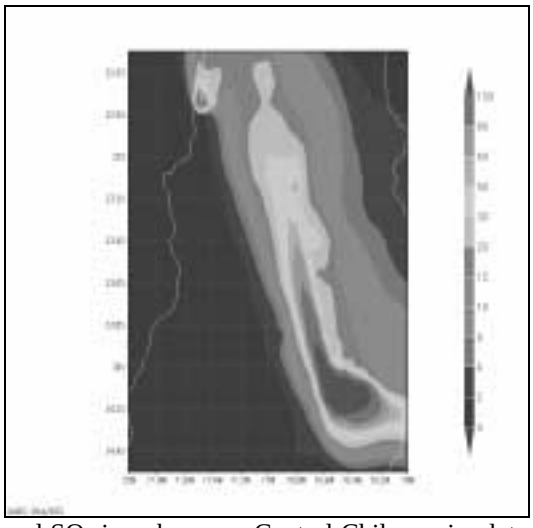

Figure 3.4-5. Vertically averaged SO_2 in ppbv, over Central Chile as simulated by the model for January 17 1998 according to the prevailing winds.

It must be pointed out that, of course, not all afternoon maxima in SO_2 observed in the Santiago basin and surroundings can be explained by long-range transport from the copper smelters as represented in the model. Concurring explanations related to sporadic emission in the urban areas, which our emission database does not account for or to shortcomings in the representation of mixing processes cannot be ruled out. Nevertheless, the simulations help us in understanding the mechanisms that explain the episodic impact of the copper smelters on the SO_2 concentrations observed in Santiago and surrounding areas, namely long-range transport and growth of boundary layer in connection with thermally driven vertical mixing.

b) Other urban areas

As it was already pointed out, outside Santiago there is very little information available to compare the model results with. This makes somewhat difficult the validation of the model in those areas. Nevertheless, the so-called COSUDE project has provided valuable information at Rancagua, Valparaíso and Viña del Mar.

For Rancagua, the monthly average for January 1998 was of about 15 μg/m^3 while the modeled concentration for that month was of about 10 μg/m^3 (See Figure 3.4-8). The modeled diurnal variation is rather strong with low daytime values below 2μg/m^3 to very high nighttime concentrations above 100 μg/m3. This city is under the semi-permanent effect of the copper smelters. The largest contribution from these sources occurs in nighttime in connection with an inhibitated vertical mixing and down-slope winds. In daytime, especially in the afternoon, the concentrations are dominated by the local sources. Since the local emissions are uncertain, their contribution may be underestimated.

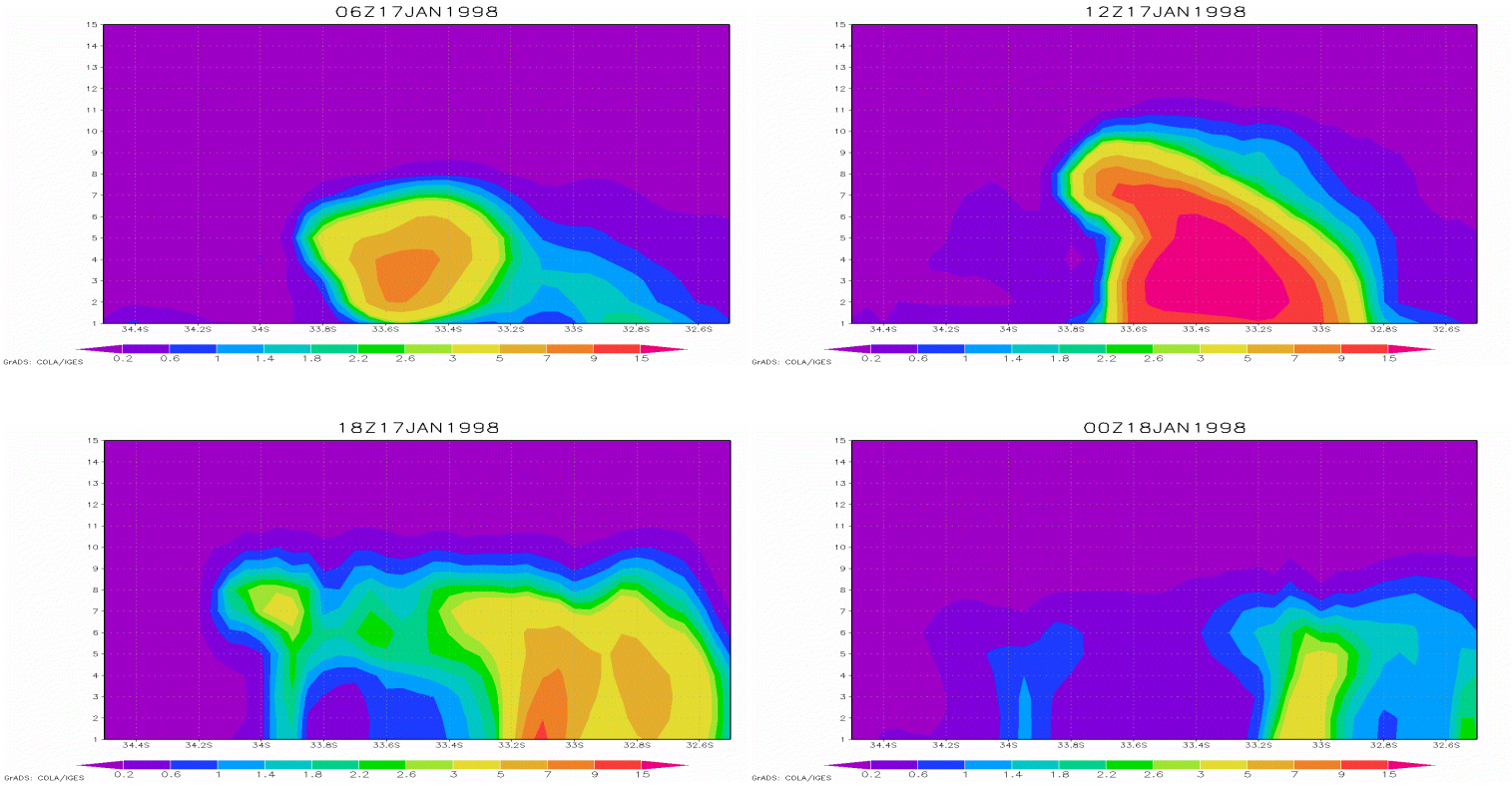

Figure 3.4-6. Vertical cross sections over Talagante during the episode of the 17th of January. The time is indicated on each figure as UTC. The scale shows SO_2 mixing ratio in ppbv.

In the Valparaíso and Viña del Mar area, local sources dominate the calculated concentrations. The effect of the copper smelters is sporadic but it increases the concentrations by a factor of four while the plume from the smelters is over the area. The model (Cf. Figure 3.4-9) underestimates by an order of magnitude the concentrations of SO_2 in Valparaíso and Viña del Mar for January 1998 (ca 35 μg/m^3). Thus, we suspect that the emission inventory for this area is underestimating the emissions. Another factor that may explain the disagreement is the rough topography we are running the model with. In fact, the model does not clearly "see" the hills that surround Valparaíso and Viña del Mar allowing much effective ventilation of the area.

Near the Ventanas copper smelter (32º44' S, 71º29' W), the reported concentrations rise up to 70 μg/m^3 while the model estimates an average concentration of 50 μg/m^3 (See

Figure 3.4-10). The diurnal cycle of the modeled concentrations shows a marked diurnal cycle associated with the sea-land breeze.

In the surroundings of the copper smelter at Chagres (32º39' S, 71º00' W), the average measured concentration is about 50 μg/m^3 while the modeled concentration is ca. 20 μg/m^3 (Cf. Figure 3.4-10**).** This difference may be related to inaccuracies in the emission inventory or the topography. The diurnal variation (not shown here) shows minimum concentrations in daytime and maximum concentrations during night according to the evolution of the boundary layer.

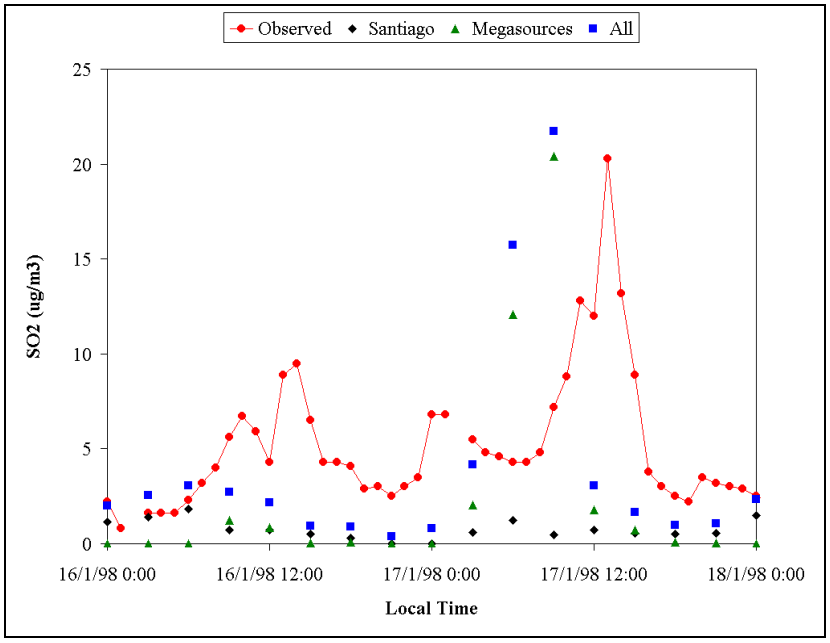

Figure 3.4-7. Time series on Talagante for the episode of January 17. The continuous line correspond to the observations and the marks to modeled results.

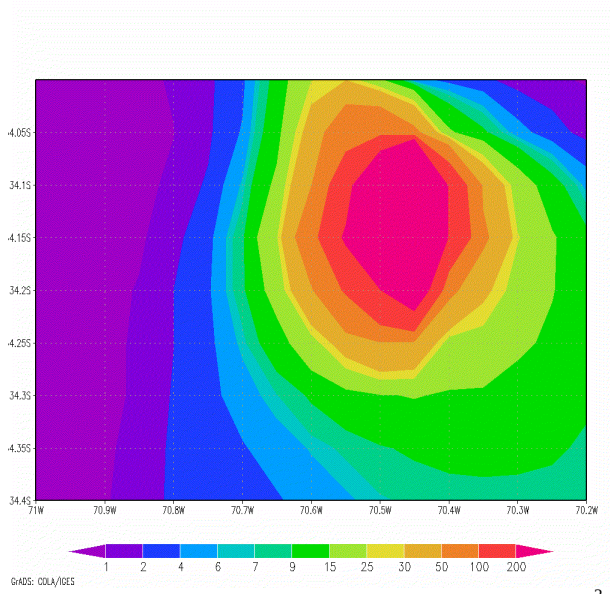

Figure 3.4-8. SO_2 average distribution in the Rancagua area. The scale is in $\mu g/m^3$.

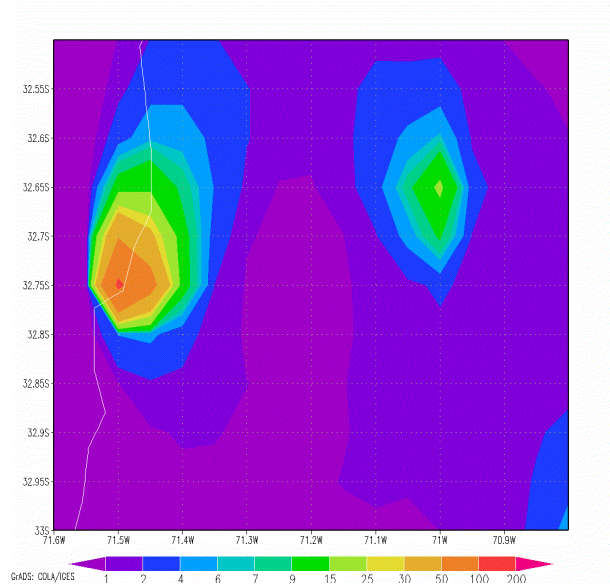

Figure 3.4-9. SO_2 average distribution in the Ventanas-Chagres area. The scale shows SO_2 concentration in $\mu g/m^3$.

3.4.4. Summary

On the regional scale, the emissions of the copper smelters dominate the oxidized sulfur burden in Central Chile. The predominance of the copper sources occurs both in horizontal and vertical distributions. The urban emissions have a modest impact, i.e., less than 10%, on the sulfur burden outside the urban areas, and above the mixed layer in comparison with the copper smelters. Moreover, the smelters contribute on an episodic basis to the sulfur burden in the urban areas.

The simulations help us in understanding the mechanisms that explain the episodic impact of the copper smelters on the SO_2 concentrations observed in Santiago and surrounding areas, namely long-range transport and growth of boundary layer in connection with thermally driven vertical mixing. Not all afternoon SO_2 maxima observed in Santiago and surrounding areas can be explained by long-range transport from the copper smelters as represented in the model. Concurring explanations related to sporadic emission in the urban areas, which our emission database does not account for or to shortcomings in the representation of mixing processes cannot be ruled out. We expect to improve these simulations as the soil information is improved allowing a better representation of latent and sensible heat fluxes in nighttime.

The model simulations are generally consistent with the observations outside the Santiago area. Rancagua is regularly affected by the Caletones copper smelter, especially in nighttime under conditions of inhibitated vertical mixing and down-slope winds. In the Valparaíso and Viña del Mar area, the effects of the copper smelters is sporadic but when it happens the SO_2 concentrations increase by a factor of four. A clear diurnal cycle associated with the sea-breeze circulation is apparent for the plume of the Ventanas copper smelter. The dispersion of the emissions from the Chagres copper smelter are strongly modulated by the up and down-slope winds in the area.

4. CONCLUSIONS AND PERSPECTIVES

A first attempt to assess the regional dispersion of pollutants in Central Chile has been presented. This corresponds to a summer case for January 1998. The modeling tool (HIRLA-MATCH) has shown able to reproduce the major features of the atmospheric circulation in the area. In addition, the calculated concentrations of sulfur dioxide and carbon monoxide are generally consistent with the available observations. However, the monitoring stations available are not designed for assessing regional dispersion patterns but mainly health effects in urban areas and local impacts of large copper smelters. Hence, a regional model with a rather coarse resolution (5x5 km^2) cannot be expected to reproduce local measurements on short time scales (minutes to hours). Nevertheless, the validation exercise so far shows consistently that the model (HIRLAM-MATCH) is able to reproduce the regional patterns of dispersion and a rather accurate picture can be obtained by applying average emission scenarios. However, a more detailed emission inventory is required for assessing local effects. Further, detailed land-use data must be incorporated in order to better simulate vertical mixing processes in the boundary layer. This is particularly important for assessing the fumigation of pollutants from aloft in connection with the strong vertical mixing that occurs in the afternoons in summer.

On the regional scale, the emissions of the copper smelters dominate the oxidized sulfur burden in Central Chile. The simulations indicate that long-range transport and growth of boundary layer in connection with thermally driven vertical mixing are important mechanisms in explaining the episodic impact of the copper smelters on the SO_2 concentrations observed in Santiago and surrounding areas. Also, a recycling of the urban emissions related to the air movements caused by the up and down-slope winds driven by radiation is apparent from the simulations. Accordingly with the prevailing winds, during daytime the large primary emissions of pollutants (e.g., CO) that take place in Central Santiago are transported towards and accumulated in Eastern Santiago. During night, when the winds turn to down-slope winds, the pollutants are transported westwards.

To continue the systematic validation of the modeling tool we are going to simulate scenarios for June 1997, May 1998 and September 1999. These scenarios will test the model's performance under conditions of subsynoptical disturbances such as coastal lows and large-scale disturbances such as frontal passages. Also, the September scenario will allow us to test more throrouly the chemical modules since observation of both gases and aerosols will be available for that period.

5. REFERENCES

Aceituno, P., 1988: On the functioning of the southern oscillation in the South American sector: part I surface climate. *Mon. Wea. Rev*., 116, 3, 505-524.

Artaxo, P., 1998: Aerosol characterization study in Santiago de Chile wintertime 1998. Part of the study:"Caracterización Físicoquimica del Material Particulado Inorgánico Primario. Distribución por Tamaño y Modelo Receptor". Comisión Nacional del Medio Ambiente, Región Metropolitana de Santiago.

Bott, A., 1989. "A Positive Definite Advective Scheme Obtained by Nonlinear Renormalization of Advective Fluxes". *Mon. Wea. Rev*., 117, 1006-1015.

Crutzen, P., 1995: Ozone in the troposphere. In "*Composition, chemistry and climate of the atmosphere*" (Singh, ed.). Van Nostrand Reinold Pub., New York, pp.349-393.

CONAMA-RM, 1997: Plan de prevención y descontaminación atmosférica de la Región Metropolitana. Comisión Nacional del Medio Ambiente, Región Metropolitana de Santiago.

García-Huidobro, T., 1999: A risk assessment of potential crop losses due to air pollution in central regions of Chile. M.Sc. Thesis. Imperial College of science, Technology and Medicine, University of London.

Jadrijevic et al, 1999: "Estudio de la calidad del aire en regiones urbano industriales de Chile". Informe final, fase intermedia. Comisión Nacional del Medio Ambiente, Departamento de Descontaminación, Planes y Normas.

Kanakidou, M. and Crutzen, P., 1999: The photochemical source of carbon monoxide: importance, uncertainties and feedbacks. *Chemosphere*, 91-109

Langner, J., Bergström, R. and Pleijel, K., 1998. "European Scale Modeling of Sulfur, Oxidized Nitrogen and Photochemical Oxidants. Model Development and Evaluation for the 1994 Growing Season". SMHI RMK Report Nº82.

REF_As, 1998: *Norma para la regulación del contaminante arsénico emitido al aire*. Expediente Público, *Rol: NOR 04/96.* Comisión Nacional del Medio Ambiente, Departamento de Descontaminación, Planes y Normas.

Robertson, L., Langner, J., Engardt, M., 1996: MATCH-Meso-scale Atmospheric Transport and Chemistry modelling system. Basic transport model description and control experiments with ^{222}Rn. Swedish Meteorological and Hydrological Institute, *RMK-70*.

Robertson, L., Langner, J., and Engardt, M. 1999: An eulerian limited-area atmospheric transport model. *J. Appl. Met*. 38, 190-210.

Rutllant, J. and Garreaud, R., 1995: Meteorological air pollution potential for Santiago Chile: towards an objective episode forecasting. *Env. Monitoring and Assessment*, 34: 223-244.

Seinfeld, J and Pandis, S., 1998: Atmospheric Chemistry and Physics. From air pollution to climate change. Chapter 9 Thermodynamics of aerosols. J. Wiley and Sons, Inc.

Tarrasón, L and Iversen, T., 1998: Modelling intercontinental transport of atmospheric sulphur in the northern hemisphere. *Tellus* 50B, 331-352.

Törnevik, H., 1993: Computer Aided Air Quality Management System. An integrated Concept including Mapping, Monitoring and Modelling in Urban Areas. National Workshop on Urban Air Quality Monitoring and Modelling. Bangalore, India.

6. INDEX